

# Enhanced Suppression of Chain Transfer in Ethylene (Co)Polymerization via Synergistic Axial Substituent Effects in Pyridine-Imine Ni(II) and Pd(II) Catalysts

Huijun Fan<sup>† a,b</sup>, Mengya Ma<sup>† a,b</sup>, Shengyu Dai<sup>\* a,b</sup>

<sup>a</sup>*School of Chemistry and Materials Science, Anhui Normal University, Wuhu 241002, China.*

<sup>b</sup>*Institutes of Physical Science and Information Technology, Anhui University, Hefei, Anhui, 230601, China.*

<sup>†</sup>The first two authors are equal first authors.

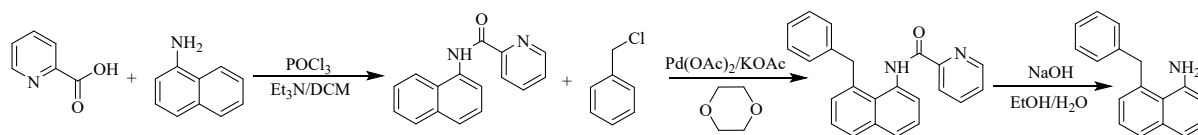
## 1. Experimental Sections

### 1.1 General Considerations

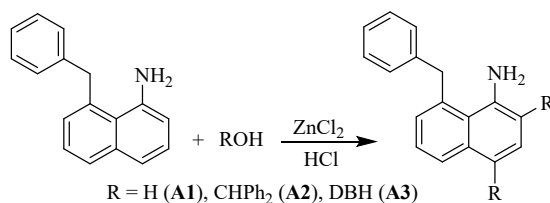
All chemicals were commercially sourced, except those whose synthesis is described. All experiments were carried out under a dry nitrogen atmosphere using standard Schlenk techniques or in a glove-box. Deuterated solvents used for NMR were dried and distilled prior to use. <sup>1</sup>H and <sup>13</sup>C NMR spectra were recorded by a JEOL JNM-ECZ600R 600 or 400 spectrometer at ambient temperature unless otherwise stated. The chemical shifts of the <sup>1</sup>H and <sup>13</sup>C NMR spectra were referenced to the residual solvent; Coupling constants are in Hz. Mass spectra and elemental analysis were performed by the Analytical Center of the Anhui University. X-ray Diffraction data were collected at 293(2) K on a Bruker Smart CCD area detector with graphite-monochromated Mo K $\alpha$  radiation ( $\lambda = 0.71073$  Å). Molecular weight and molecular weight distribution of the polymers with low solubility at room temperature were determined by gel permeation chromatography (GPC) with a PL 210 equipped with one Shodex AT-803S and two Shodex AT-806MS columns at 150 °C using trichlorobenzene as a solvent and calibrated with polystyrene standards. The molecular weight and the molecular weight distribution of the polymers with good solubility at room temperature were determined by gel permeation chromatography (GPC) equipped with two linear Styragel columns (HR2 and HR4) at 40 °C using THF as a solvent and calibrated with polystyrene standards, and THF was employed as the eluent at a flow rate of 1.0 mL/min. Differential scanning calorimetry (DSC) was performed by a DSC Q25 from TA Instruments. Samples were quickly heated to 150 °C and kept for 5 min to remove thermal history, then cooled to -50 °C at a rate of 10

K/min, and finally reheated to 150 °C at the same rate under a nitrogen flow (50 mL/min). The maximum points endotherm (heating scan) were taken as the melting temperature ( $T_m$ ).

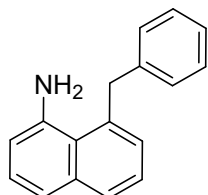
## 1.2 Procedure for the Synthesis of Arylamines A1-A3.



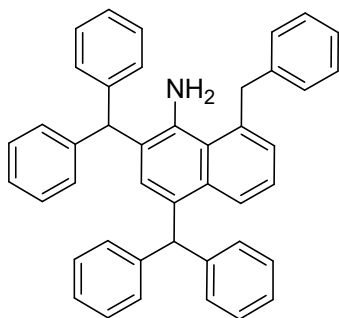
The key intermediate, 8-benzyl-1-naphthylamine, was synthesized via directed C–H functionalization at the 8-position of naphthylamine using a pyridylcarbonyl directing group, followed by its removal according to literature procedures.<sup>1</sup>



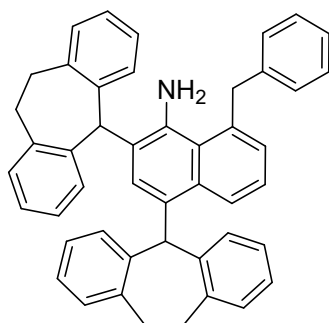
In a typical reaction, a mixture of 8-benzyl-1-naphthylamine (10 mmol, 1.0 equiv.) and either diphenylmethanol or dibenzosuberol (20.0 mmol, 2.0 equiv.) was heated to 120 °C under an inert atmosphere, followed by dropwise addition of a solution of anhydrous zinc chloride (1.36 g, 10 mmol, 0.5 equiv.) in concentrated hydrochloric acid (1.2 mL, 37% w/w, 1.0 equiv.), during which exothermic and intense bubbling were observed. The temperature was then raised to 160 °C and maintained for 30 min. After cooling to room temperature, the mixture was dissolved in CH<sub>2</sub>Cl<sub>2</sub> (200 mL), washed with water (3 × 100 mL), and dried over anhydrous MgSO<sub>4</sub>. The solution was concentrated to ~20 mL under reduced pressure, and the product was precipitated by addition to methanol (200 mL). The resulting solid was collected by filtration and washed with cold methanol (3 × 100 mL) to afford the pure product.



**A1** (0.96 g, 41%, two steps). **A1** is known.<sup>1</sup>

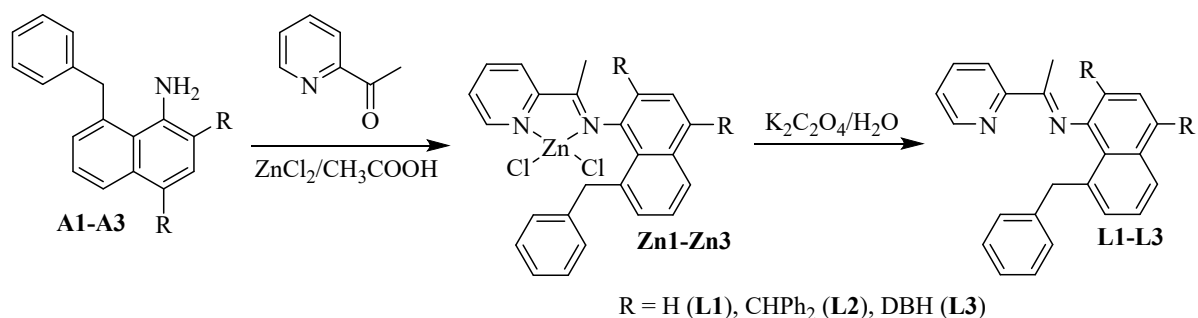


**A2** (1.81 g, 32%).  $^1\text{H}$  NMR (400 MHz,  $\text{CDCl}_3$ )  $\delta$  7.85 (d,  $J$  = 8.5 Hz, 1H, Ar-*H*), 7.37 – 7.04 (m, 19H, Ar-*H*), 7.02 – 6.71 (m, 8H, Ar-*H*), 6.31 (s, 1H, Ar-*H*), 6.03 (s, 1H, CHAr<sub>2</sub>), 5.46 (s, 1H, CHAr<sub>2</sub>), 4.68 (s, 2H, -CH<sub>2</sub>-), 3.93 (s, *br*, 2H, NH<sub>2</sub>).  $^{13}\text{C}$  NMR (101 MHz,  $\text{CDCl}_3$ )  $\delta$  144.21, 142.54, 141.01, 140.19, 134.68, 133.31, 130.81, 130.38, 129.41, 129.30, 128.91, 128.60, 128.40, 128.16, 126.48, 126.44, 125.97, 125.64, 125.12, 123.75, 122.76, 53.32 (CHAr<sub>2</sub>), 52.18 (CHAr<sub>2</sub>), 42.27 (-CH<sub>2</sub>-). APCI-MS ( $m/z$ ): calcd for  $\text{C}_{43}\text{H}_{36}\text{N}$ : 566.2842, Found, 566.2859,  $[\text{M}+\text{H}]^+$ .



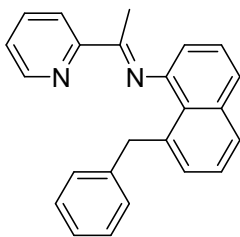
**A3** (1.79 g, 29%).  $^1\text{H}$  NMR (400 MHz,  $\text{CDCl}_3$ )  $\delta$  8.26 (d,  $J$  = 8.6 Hz, 1H, Ar-*H*), 7.40 (d,  $J$  = 6.9 Hz, 2H, Ar-*H*), 7.30 – 7.22 (m, 5H, Ar-*H*),  $\delta$  7.21 – 7.02 (m, 12H, Ar-*H*), 6.96 (s, 1H, Ar-*H*), 6.90 (dd,  $J$  = 14.5, 7.1 Hz, 4H, Ar-*H*), 5.69 (s, 1H, CHAr<sub>2</sub>), 5.07 (s, 1H, CHAr<sub>2</sub>), 4.61 (s, 2H, -CH<sub>2</sub>-), 4.19 (s, 2H, *br*, 2H, NH<sub>2</sub>), 2.82 – 2.62 (m, 4H, -CH<sub>2</sub>-CH<sub>2</sub>-), 2.44 – 2.26 (m, 4H, -CH<sub>2</sub>-CH<sub>2</sub>-).  $^{13}\text{C}$  NMR (101 MHz,  $\text{CDCl}_3$ )  $\delta$  141.10, 140.41, 140.24, 140.17, 140.05, 134.76, 133.15, 132.92, 131.15, 130.94, 130.87, 130.09, 128.85, 128.61, 127.45, 127.10, 126.62, 126.40, 126.21, 126.07, 125.92, 124.69, 124.05, 121.78, 57.22 (CHAr<sub>2</sub>), 56.60 (CHAr<sub>2</sub>), 42.32 (-CH<sub>2</sub>-), 31.36 (-CH<sub>2</sub>-CH<sub>2</sub>-), 31.31 (-CH<sub>2</sub>-CH<sub>2</sub>-). APCI-MS ( $m/z$ ): calcd for  $\text{C}_{47}\text{H}_{36}\text{N}$ : 614.2842, Found, 614.2844,  $[\text{M}-4\text{H}+\text{H}]^+$ .

### 1.3 Procedure for the Synthesis of Ligands L1-L3.

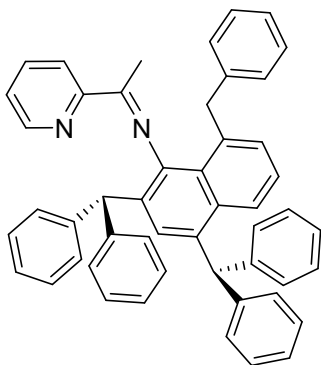


The ligands **L1–L3** were synthesized via a two-step procedure. First, a suspension of ZnCl<sub>2</sub> (0.34 g, 2.5 mmol) and 2-acetylpyridine (2.0 mmol) in glacial acetic acid (5 mL) was treated with the corresponding aniline **A1–A3** (2 mmol). The reaction mixture was refluxed with stirring for 4 h, yielding a yellow precipitate upon cooling to room temperature. The solid was isolated by filtration and thoroughly washed with acetic acid (3 × 5 mL) followed by diethyl ether (5 × 5 mL) to remove residual acetic acid. Drying under vacuum afforded the zinc-iminopyridine complex as a yellow, poorly soluble solid.

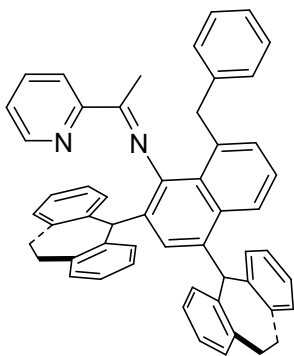
Subsequent demetallation was achieved by suspending the zinc complex in methylene chloride (30 mL) and adding an aqueous solution of potassium oxalate (0.41 g, 2.2 mmol in 5 mL H<sub>2</sub>O). The biphasic mixture was vigorously stirred for 1 h, after which the organic layer was separated, washed with water (3 × 20 mL), and dried over MgSO<sub>4</sub>. Filtration and solvent removal under reduced pressure yielded a crude product, which was further purified by precipitation from ethanol (20 mL). Ligands **L2** and **L3** were obtained as stable yellow powders after drying under high vacuum. However, **L1** proved unstable and prone to decomposition in solution, precluding the acquisition of pure NMR spectroscopic data.



**L1** (0.29 g, 63%). **L1** exhibits instability in solution, precluding the acquisition of pure NMR spectroscopic data. APCI-MS (*m/z*): calcd for C<sub>24</sub>H<sub>21</sub>N<sub>2</sub>: 337.1699, Found, 337.1701, [M+H]<sup>+</sup>.



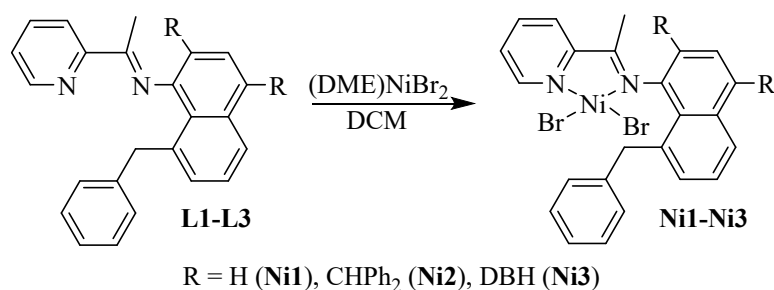
**L2** (1.02 g, 76%).  $^1\text{H}$  NMR (600 MHz,  $\text{CDCl}_3$ )  $\delta$  8.54 (d,  $J = 4.3$  Hz, 1H, Ar-*H*), 8.28 (d,  $J = 8.0$  Hz, 1H, Ar-*H*), 7.93 (d,  $J = 8.5$  Hz, 1H, Ar-*H*), 7.82 – 7.72 (m, 1H, Ar-*H*), 7.34 (dd,  $J = 6.9, 5.4$  Hz, 1H, Ar-*H*), 7.28 – 7.24 (m, 4H, Ar-*H*), 7.22 – 7.16 (m, 3H, Ar-*H*), 7.15 – 7.09 (m, 4H, Ar-*H*), 7.08 – 7.02 (m, 6H, Ar-*H*), 7.02 – 6.98 (m, 4H, Ar-*H*), 6.87 – 6.83 (m, 2H, Ar-*H*), 6.82 – 6.77 (m, 2H, Ar-*H*), 6.72 (d,  $J = 7.4$  Hz, 2H, Ar-*H*), 6.69 (s, 1H, Ar-*H*), 6.19 (s, 1H,  $\text{CHAr}_2$ ), 5.40 (s, 1H,  $\text{CHAr}_2$ ), 4.50 (d,  $J = 16.5$  Hz, 1H,  $-\text{CH}_2-$ ), 4.28 (d,  $J = 16.5$  Hz, 1H,  $-\text{CH}_2-$ ), 1.17 (s, 3H,  $\text{Ar-C}(\text{CH}_3)=\text{N}$ ).  $^{13}\text{C}$  NMR (151 MHz,  $\text{CDCl}_3$ )  $\delta$  167.70 ( $\text{C}=\text{N}$ ), 155.73, 148.43, 145.46, 144.34, 143.95, 143.80, 142.37, 141.45, 136.84, 136.12, 134.63, 132.79, 130.66, 129.92, 129.62, 129.49, 129.18, 128.91, 128.35, 128.30, 128.24, 127.95, 127.89, 126.52, 126.28, 126.19, 126.13, 125.89, 125.59, 125.39, 124.71, 123.20, 121.24, 53.49 ( $\text{CHAr}_2$ ), 52.07 ( $\text{CHAr}_2$ ), 42.43 ( $-\text{CH}_2-$ ), 16.92 ( $\text{Ar-C}(\text{CH}_3)=\text{N}$ ). APCI-MS ( $m/z$ ): calcd for  $\text{C}_{50}\text{H}_{41}\text{N}_2$ : 669.3264, Found, 669.3259,  $[\text{M}+\text{H}]^+$ .



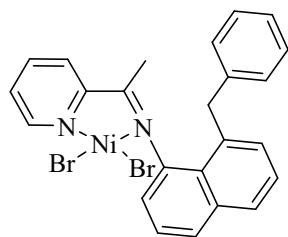
**L3** (1.02 g, 71%).  $^1\text{H}$  NMR (400 MHz,  $\text{CDCl}_3$ )  $\delta$  8.55 (d,  $J = 4.0$  Hz, 1H, Ar-*H*), 8.31 (d,  $J = 8.6$  Hz, 2H, Ar-*H*), 7.80 (td,  $J = 7.8, 1.7$  Hz, 1H, Ar-*H*), 7.55 – 7.43 (m, 2H, Ar-*H*), 7.40 – 7.34 (m, 1H, Ar-*H*), 7.29 – 7.10 (m, 8H, Ar-*H*), 7.02 – 6.89 (m, 9H, Ar-*H*), 6.84 (t,  $J = 7.4$  Hz, 2H, Ar-*H*), 6.67 – 6.59 (m, 3H, Ar-*H*), 5.82 (s, 1H,  $\text{CHAr}_2$ ), 5.03 (s, 1H,  $\text{CHAr}_2$ ), 4.44 (d,  $J = 16.6$  Hz, 1H,  $-\text{CH}_2-$ ), 4.21 (d,  $J = 16.6$  Hz, 1H,  $-\text{CH}_2-$ ), 2.87 – 2.58 (m, 4H,  $-\text{CH}_2-\text{CH}_2-$ ), 2.52 – 2.29 (m, 4H,  $-\text{CH}_2-\text{CH}_2-$ ), 1.31 (s, 3H,  $\text{Ar-C}(\text{CH}_3)=\text{N}$ ).  $^{13}\text{C}$  NMR (101 MHz,  $\text{CDCl}_3$ )  $\delta$  167.29

(C=N), 155.41, 148.25, 145.23, 141.39, 141.06, 140.95, 140.44, 140.29, 140.25, 140.07, 139.93, 139.63, 136.75, 135.88, 132.50, 132.07, 131.62, 131.51, 131.12, 130.98, 130.92, 130.80, 130.70, 130.46, 129.67, 128.81, 127.59, 126.88, 126.84, 126.76, 126.62, 126.07, 125.99, 125.66, 125.37, 125.32, 124.88, 124.67, 124.39, 123.40, 121.66, 57.41 (CHAr<sub>2</sub>), 56.34 (CHAr<sub>2</sub>), 42.54 (-CH<sub>2</sub>-), 31.63 (-CH<sub>2</sub>-CH<sub>2</sub>-), 31.54 (-CH<sub>2</sub>-CH<sub>2</sub>-), 31.32 (-CH<sub>2</sub>-CH<sub>2</sub>-), 31.16 (-CH<sub>2</sub>-CH<sub>2</sub>-), 16.31 (Ar-C(CH<sub>3</sub>)=N). APCI-MS (m/z): calcd for C<sub>54</sub>H<sub>45</sub>N<sub>2</sub>: 721.3577, Found, 721.3564, [M+H]<sup>+</sup>.

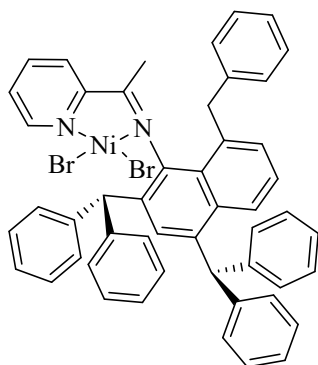
#### 1.4 Procedure for the Synthesis of Nickel Complexes Ni1-Ni3.



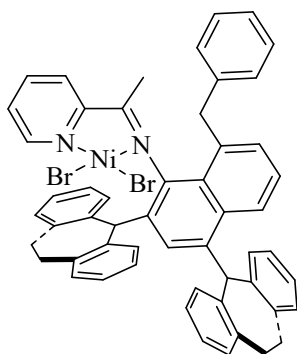
Complexes **Ni1-Ni3** were synthesized by reacting (DME)NiBr<sub>2</sub> with the corresponding ligands in methylene chloride under nitrogen atmosphere. In a typical procedure, the ligand (0.2 mmol) was dissolved in methylene chloride (5 mL) in a Schlenk tube. (DME)NiBr<sub>2</sub> (0.2 mmol, 62 mg) was then added to the solution, and the resulting mixture was stirred at room temperature for 12 hours. After removal of the solvent under reduced pressure, the solid product was washed with diethyl ether (4 × 5 mL) and dried in vacuo.



**Ni1**: (92 mg, 83%). Elemental analysis: calc. for C<sub>24</sub>H<sub>20</sub>Br<sub>2</sub>N<sub>2</sub>Ni: C, 51.95; H, 3.63; N, 5.05. Found: C, 51.87; H, 3.65; N, 5.12.

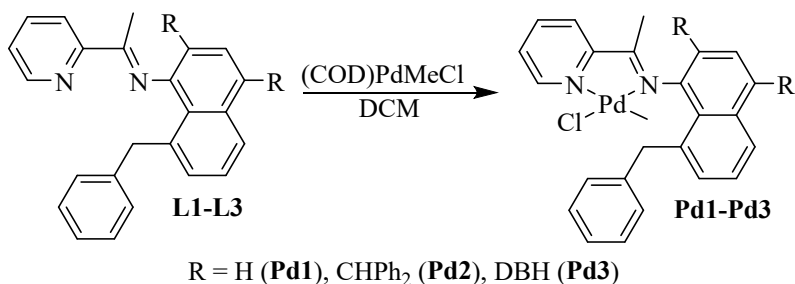


**Ni2:** (162 mg, 91%). Elemental analysis: calc. for  $C_{50}H_{40}Br_2N_2Ni$ : C, 67.68; H, 4.54; N, 3.16. Found: C, 67.54; H, 4.36; N, 3.28.

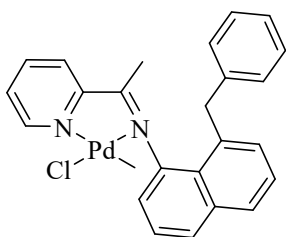


**Ni3:** (169 mg, 90%). Elemental analysis: calc. for  $C_{54}H_{44}Br_2N_2Ni$ : C, 69.04; H, 4.72; N, 2.98. Found: C, 69.21; H, 4.77; N, 2.89.

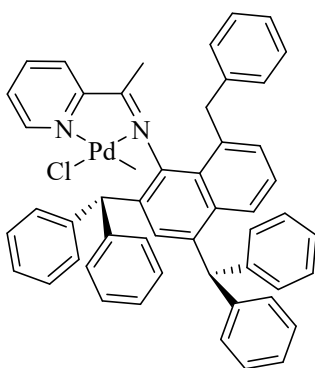
### 1.5 Procedure for the Synthesis of Palladium Complexes Pd1-Pd3.



A solution of the ligand (0.5 mmol) and (COD)PdMeCl (133 mg, 0.5 mmol) in dichloromethane (20 mL) was stirred at room temperature for 12 h. During the reaction, the solution gradually darkened in color. After completion, the mixture was concentrated to ~2 mL under reduced pressure, and the product was precipitated by addition of diethyl ether (20 mL). The resulting solid was collected, washed with additional diethyl ether (3 × 5 mL), and dried *in vacuo* for 1 h to afford the pure compound as a yellow solid.



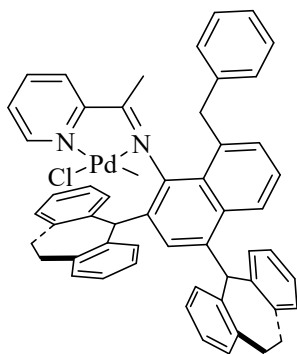
**Pd1:** (200 mg, 81%).  $^1\text{H}$  NMR (400 MHz,  $\text{CDCl}_3$ )  $\delta$  9.26 (d,  $J = 5.0$  Hz, 1H, Ar-*H*), 7.92 (td,  $J = 7.8, 1.3$  Hz, 1H, Ar-*H*), 7.87 (d,  $J = 8.1$  Hz, 1H, Ar-*H*), 7.81 (d,  $J = 8.1$  Hz, 1H, Ar-*H*), 7.68 (dd,  $J = 7.6, 5.2$  Hz, 1H, Ar-*H*), 7.51 (q,  $J = 6.9$  Hz, 1H, Ar-*H*), 7.48 – 7.40 (m, 1H, Ar-*H*), 7.36 (d,  $J = 6.9$  Hz, 1H, Ar-*H*), 7.29 (d,  $J = 7.9$  Hz, 1H, Ar-*H*), 6.96 (t,  $J = 7.3$  Hz, 1H, Ar-*H*), 6.84 – 6.74 (m, 3H, Ar-*H*), 6.55 (d,  $J = 7.6$  Hz, 2H, Ar-*H*), 6.26 (d,  $J = 17.2$  Hz, 1H,  $-\text{CH}_2-$ ), 4.30 (d,  $J = 17.2$  Hz, 1H,  $-\text{CH}_2-$ ), 1.31 (s, 3H, Ar- $\text{C}(\text{CH}_3)=\text{N}$ ), 0.45 (s, 3H, Pd- $\text{CH}_3$ ).  $^{13}\text{C}$  NMR (101 MHz,  $\text{CDCl}_3$ )  $\delta$  173.80 ( $\text{C}=\text{N}$ ), 153.41, 149.11, 144.76, 141.75, 138.28, 136.36, 133.92, 132.96, 128.71, 128.59, 128.13, 126.85, 126.49, 125.83, 125.12, 124.95, 120.28, 42.72 ( $-\text{CH}_2-$ ), 18.65 ( $\text{C}(\text{CH}_3)=\text{N}-\text{Ar}$ ), -0.36 (Pd- $\text{CH}_3$ ). Key  $^{13}\text{C}$  and  $^1\text{H}$  HSQC correlations ( $\text{CDCl}_3$ ): 18.65 ( $\text{C}(\text{CH}_3)=\text{N}-\text{Ar}$ )/1.31 (s, 3H, Ar- $\text{C}(\text{CH}_3)=\text{N}$ ); -0.36 (Pd- $\text{CH}_3$ )/0.45 (s, 3H, Pd- $\text{CH}_3$ ). Elemental analysis: calc. for  $\text{C}_{25}\text{H}_{23}\text{ClN}_2\text{Pd}$ : C, 60.87; H, 4.70; N, 5.68. Found: C, 60.78; H, 4.69; N, 5.74.



**Pd2:** (363 mg, 88%). a-isomer: b-isomer = 10:1  $^1\text{H}$  NMR (400 MHz,  $\text{CDCl}_3$ )  $\delta$  9.56, 9.33 (d,  $J = 5.4$  Hz, 1H, Ar-*H*), 8.02, 7.94 (d,  $J = 8.4$  Hz, 1H, Ar-*H*), 7.74 (td,  $J = 7.8, 1.5$  Hz, 1H, Ar-*H*), 7.63 (dd,  $J = 14.9, 8.0$  Hz, 1H, Ar-*H*), 7.44 – 7.38 (m, 1H, Ar-*H*), 7.31 (d,  $J = 7.0$  Hz, 1H, Ar-*H*), 7.25 (d,  $J = 6.0$  Hz, 4H, Ar-*H*), 7.14 (dd,  $J = 13.1, 7.0$  Hz, 3H, Ar-*H*), 6.89 – 6.83 (m, 5H, Ar-*H*), 6.94 (d,  $J = 6.9$  Hz, 3H, Ar-*H*), 6.88 – 6.82 (m, 6H, Ar-*H*), 6.72 (dd,  $J = 14.5, 7.0$  Hz, 5H, Ar-*H*), 6.62 (dd,  $J = 9.8, 5.8$  Hz, 1H, Ar-*H*), 6.49 (s, 1H,  $\text{CHAr}_2$ ), 6.20 (s, 1H,  $\text{CHAr}_2$ ), 6.10 (d,  $J = 17.1$  Hz, 1H,  $-\text{CH}_2-$ ), 4.52, 4.35 (d,  $J = 17.6$  Hz, 1H,  $-\text{CH}_2-$ ), 0.78, 0.71 (s, 3H,  $\text{C}(\text{CH}_3)=\text{N}-\text{Ar}$ ), 0.22, 0.17 (s, 3H, Pd- $\text{CH}_3$ ).  $^{13}\text{C}$  NMR (101 MHz,  $\text{CDCl}_3$ )  $\delta$  176.17 ( $\text{C}=\text{N}$ ),



153.12, 148.86, 143.88, 142.91, 142.22, 141.06, 140.26, 140.08, 139.00, 137.89, 134.00, 133.52, 133.05, 132.29, 130.53, 130.29, 129.56, 129.33, 129.08, 128.57, 128.53, 128.43, 128.11, 127.77, 127.70, 126.59, 126.55, 126.42, 126.32, 125.97, 125.85, 124.32, 123.94, 53.68 ( $\text{CHAr}_2$ ), 52.42 ( $\text{CHAr}_2$ ), 42.59 ( $-\text{CH}_2-$ ), 18.17 ( $\text{Ar-C}(\text{CH}_3)=\text{N}$ ), 1.44 ( $\text{Pd-CH}_3$ ). Elemental analysis: calc. for  $\text{C}_{51}\text{H}_{43}\text{ClN}_2\text{Pd}$ : C, 74.18; H, 5.25; N, 3.39. Found: C, 74.24; H, 5.36; N, 3.43.



**Pd3:** (395 mg, 90%). a-isomer: b-isomer = 10:1.  $^1\text{H}$  NMR (400 MHz,  $\text{CDCl}_3$ )  $\delta$  9.57, 9.35 (d,  $J = 4.8$  Hz, 1H, Ar-*H*), 8.76, 8.42 (d,  $J = 8.6$  Hz, 1H, Ar-*H*), 7.68 (t,  $J = 7.7$  Hz, 2H, Ar-*H*), 7.65 – 7.59 (m, 1H, Ar-*H*), 7.39 (dd,  $J = 14.3, 6.0$  Hz, 2H, Ar-*H*), 7.31 – 7.27 (m, 2H, Ar-*H*), 7.25 – 7.15 (m, 6H, Ar-*H*), 7.14 – 7.05 (m, 2H, Ar-*H*), 6.92 (d,  $J = 7.2$  Hz, 2H, Ar-*H*), 6.83 (t,  $J = 6.4$  Hz, 2H, Ar-*H*), 6.78 (d,  $J = 7.4$  Hz, 2H, Ar-*H*), 6.74 – 6.66 (m, 4H, Ar-*H*), 6.53 (d,  $J = 7.7$  Hz, 1H, Ar-*H*), 6.13 (d,  $J = 17.4$  Hz, 1H,  $-\text{CH}_2-$ ), 6.07 (s, 1H,  $\text{CHAr}_2$ ), 5.95 (t,  $J = 6.9$  Hz, 1H, Ar-*H*), 5.82 (s, 1H,  $\text{CHAr}_2$ ), 4.47, 4.32 (d,  $J = 17.3$  Hz, 1H,  $-\text{CH}_2-$ ), 3.09 (td,  $J = 14.0, 4.5$  Hz, 1H,  $-\text{CH}_2-\text{CH}_2-$ ), 2.89 – 2.75 (m, 1H,  $-\text{CH}_2-\text{CH}_2-$ ), 2.68 – 2.53 (m, 2H,  $-\text{CH}_2-\text{CH}_2-$ ), 2.25 – 2.00 (m, 4H,  $-\text{CH}_2-\text{CH}_2-$ ), 0.89, 0.78 (s, 3H,  $\text{C}(\text{CH}_3)=\text{N-Ar}$ ), 0.40, 0.37 (s, 3H,  $\text{Pd-CH}_3$ ).  $^{13}\text{C}$  NMR (101 MHz,  $\text{CDCl}_3$ )  $\delta$  176.80 ( $\text{C}=\text{N}$ ), 153.39, 148.69, 142.44, 141.48, 140.99, 140.69, 140.16, 140.00, 139.39, 138.95, 137.76, 137.72, 136.44, 133.76, 133.51, 133.06, 132.89, 132.56, 132.20, 131.32, 130.69, 130.61, 130.06, 128.71, 128.65, 128.51, 128.40, 127.63, 127.58, 127.39, 127.07, 126.99, 126.87, 126.49, 126.25, 126.13, 125.77, 125.55, 125.38, 124.60, 124.41, 57.80 ( $\text{CHAr}_2$ ), 56.15 ( $\text{CHAr}_2$ ), 42.73 ( $-\text{CH}_2-$ ), 32.54 ( $-\text{CH}_2-\text{CH}_2-$ ), 32.42 ( $-\text{CH}_2-\text{CH}_2-$ ), 29.94 ( $-\text{CH}_2-\text{CH}_2-$ ), 29.41 ( $-\text{CH}_2-\text{CH}_2-$ ), 18.01 ( $\text{C}(\text{CH}_3)=\text{N-Ar}$ ), 1.27 ( $\text{Pd-CH}_3$ ). Elemental analysis: calc. for  $\text{C}_{55}\text{H}_{47}\text{ClN}_2\text{Pd}$ : C, 75.25; H, 5.40; N, 3.19. Found: C, 75.33; H, 5.44; N, 3.12.

## 1.6 A General Procedure for the Homopolymerization of Ethylene Using Ni Complexes.

In a typical experiment, a 350 mL thick-walled glass pressure reactor was dried at 90 °C under vacuum for  $\geq 1$  h. After cooling to the desired polymerization temperature, the reactor was charged with toluene (20 mL) and the appropriate amount of  $\text{Et}_2\text{AlCl}$  under a nitrogen atmosphere in a glovebox. The glass polymerization reactor was subsequently integrated into a medium-pressure polymerization line, where the catalyst (dissolved in 1 mL of  $\text{CH}_2\text{Cl}_2$ ) was injected into the system via syringe under ethylene atmosphere. Under vigorous stirring (350 rpm), the reactor was pressurized with ethylene (6 atm) and maintained at this pressure for 10 min. The reaction was then quenched by venting the reactor, and the polyethylene was precipitated by addition of ethanol. The product was isolated by filtration and dried *in vacuo* at 50 °C for  $\geq 24$  h.

### **1.7 A General Procedure for the Homopolymerization of Ethylene Using Pd Complexes.**

In a typical experiment, a 350 mL thick-walled glass pressure reactor was dried at 90 °C under vacuum for  $\geq 1$  h. After cooling to the desired polymerization temperature, the reactor was charged with toluene (38 mL) and the appropriate amount of NaBARF under a nitrogen atmosphere in a glovebox. The glass polymerization reactor was subsequently integrated into a medium-pressure polymerization line, where the Pd catalyst (dissolved in 2 mL of  $\text{CH}_2\text{Cl}_2$ ) was injected into the system via syringe under ethylene atmosphere. Under vigorous stirring (350 rpm), the reactor was pressurized with ethylene (4 atm) and maintained at this pressure for 1 h. The reaction was then quenched by venting the reactor, and the polyethylene product was isolated by rotary evaporation to remove volatile solvents and subsequently dried under vacuum.

### **1.8 A General Procedure for the Copolymerization of Methyl Acrylate with Ethylene using Pd Complexes.**

In a typical experiment, a 350 mL thick-walled glass pressure reactor was dried at 90 °C under vacuum for  $\geq 1$  h. After cooling to the desired polymerization temperature, the reactor was charged with  $\text{CH}_2\text{Cl}_2$  (18 mL) and the appropriate amount of NaBARF and MA under a nitrogen atmosphere in a glovebox. The glass polymerization reactor was subsequently integrated into a medium-pressure polymerization line, where the Pd catalyst (dissolved in 2 mL of  $\text{CH}_2\text{Cl}_2$ )

was injected into the system via syringe under ethylene atmosphere. Under vigorous stirring, the reactor was pressurized with ethylene (4 atm) and maintained at this pressure for 3 h. The reaction was then quenched by venting the reactor, and the E-MA copolymer was isolated by rotary evaporation to remove volatile solvents and subsequently dried under vacuum.

## 2. Spectra Data

### 2.1 $^1\text{H}$ and $^{13}\text{C}$ NMR of the Synthetic Compounds.

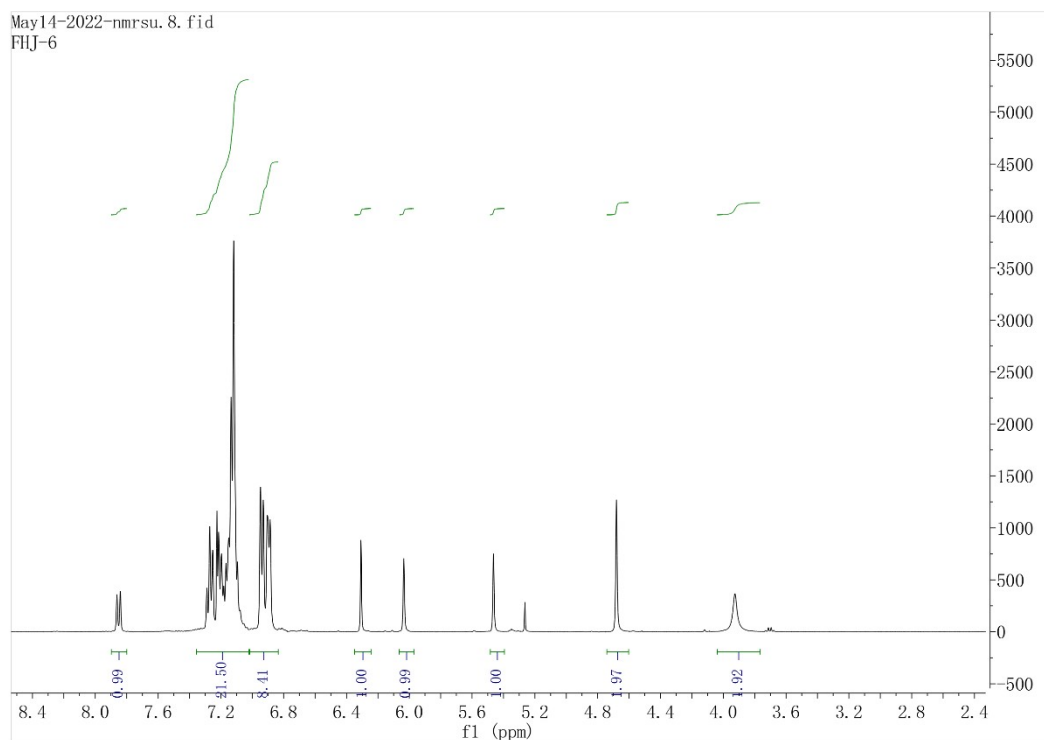


**Figure S1.**  $^1\text{H}$  NMR spectrum of **A2** in  $\text{CDCl}_3$ .

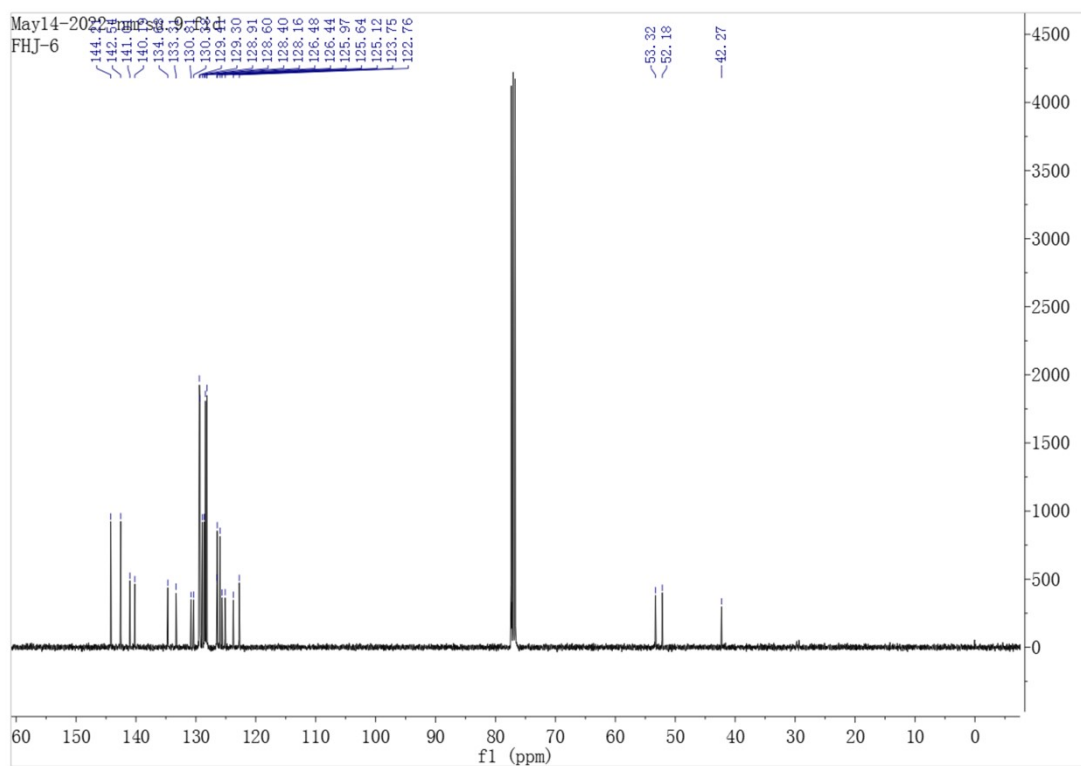


**Figure S2.**  $^{13}\text{C}$  NMR spectrum of A2 in  $\text{CDCl}_3$ .

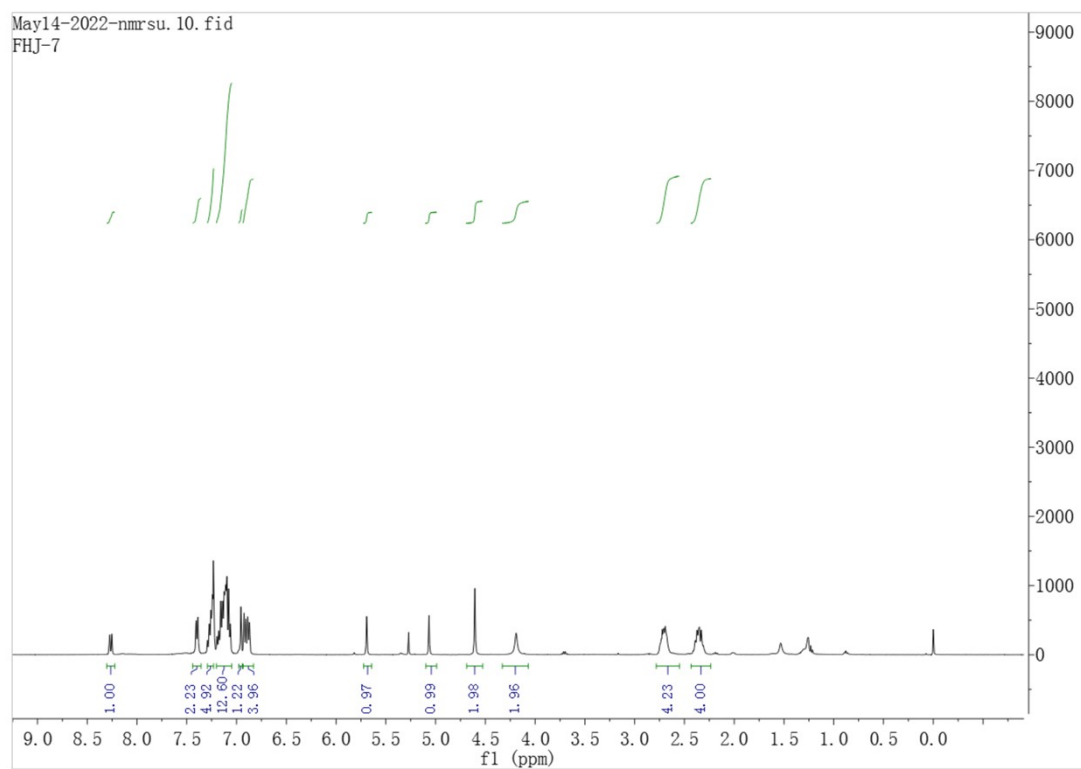


**Figure S3.**  $^1\text{H}$  NMR spectrum of A3 in  $\text{CDCl}_3$ .

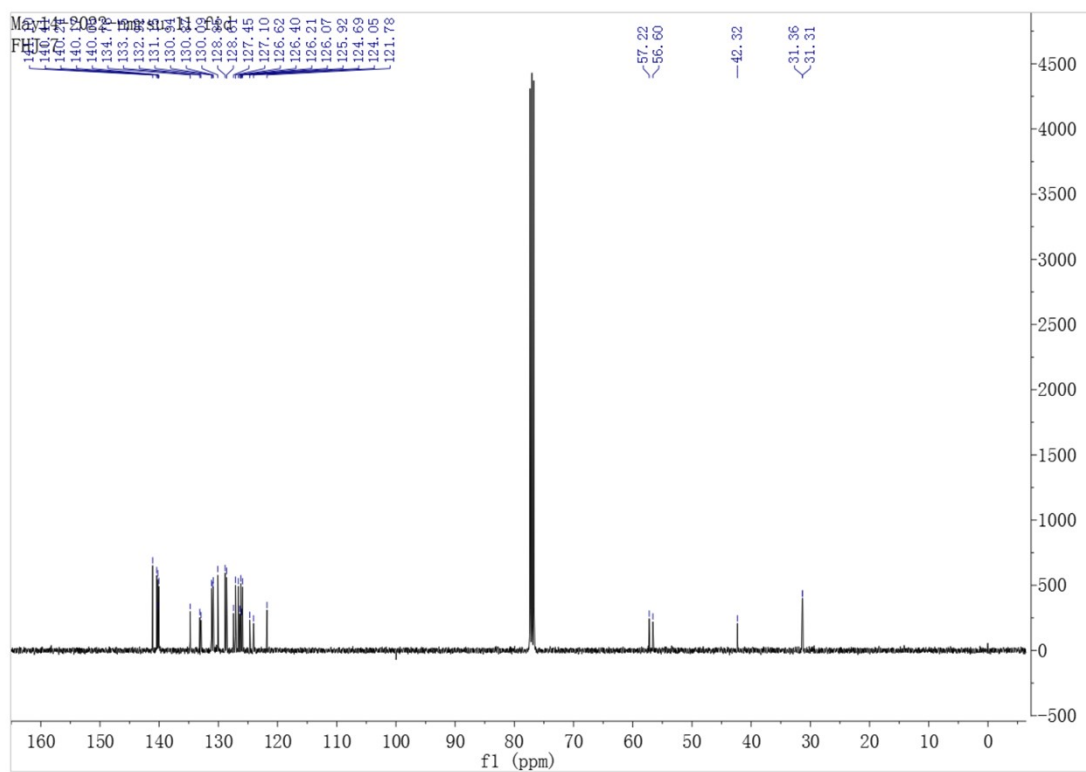


**Figure S4.**  $^{13}\text{C}$  NMR spectrum of **A3** in  $\text{CDCl}_3$ .

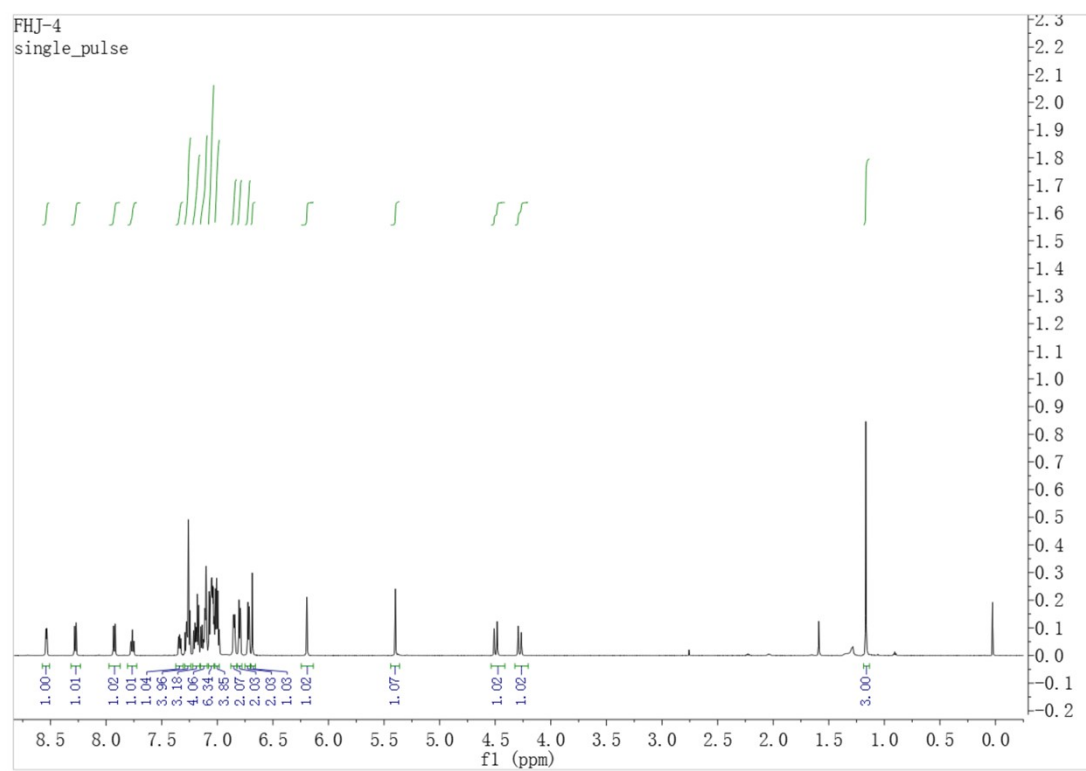


**Figure S5.**  $^1\text{H}$  NMR spectrum of **L2** in  $\text{CDCl}_3$ .

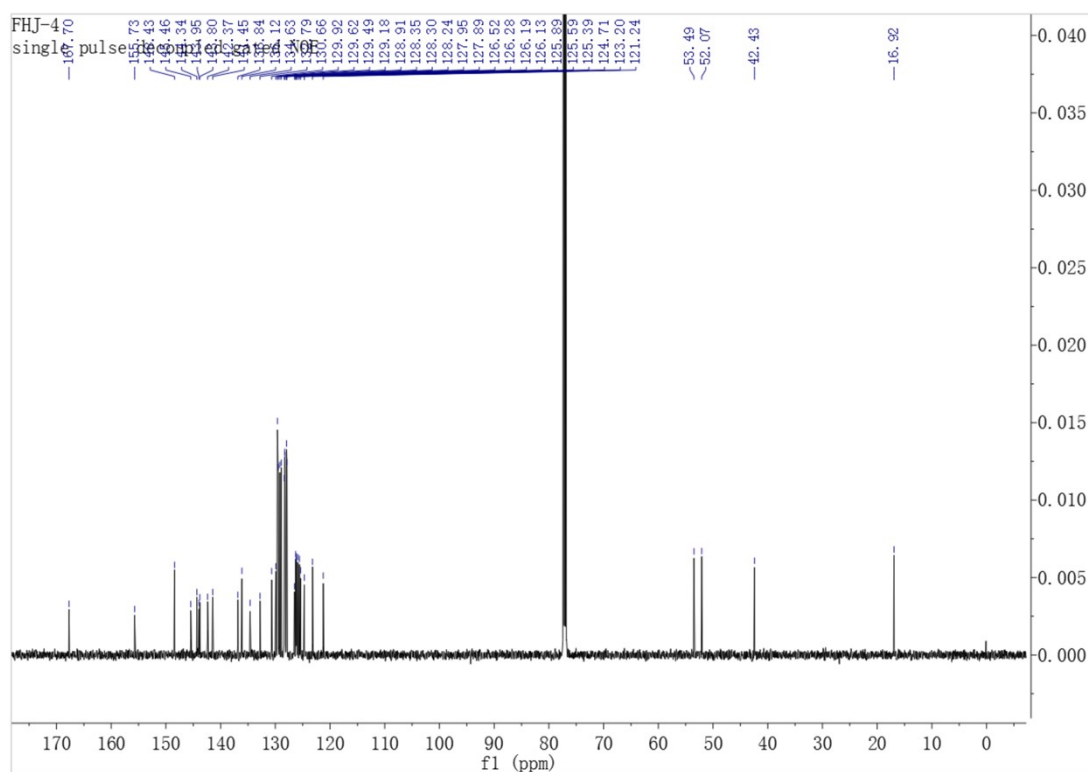


**Figure S6.**  $^{13}\text{C}$  NMR spectrum of **L2** in  $\text{CDCl}_3$ .

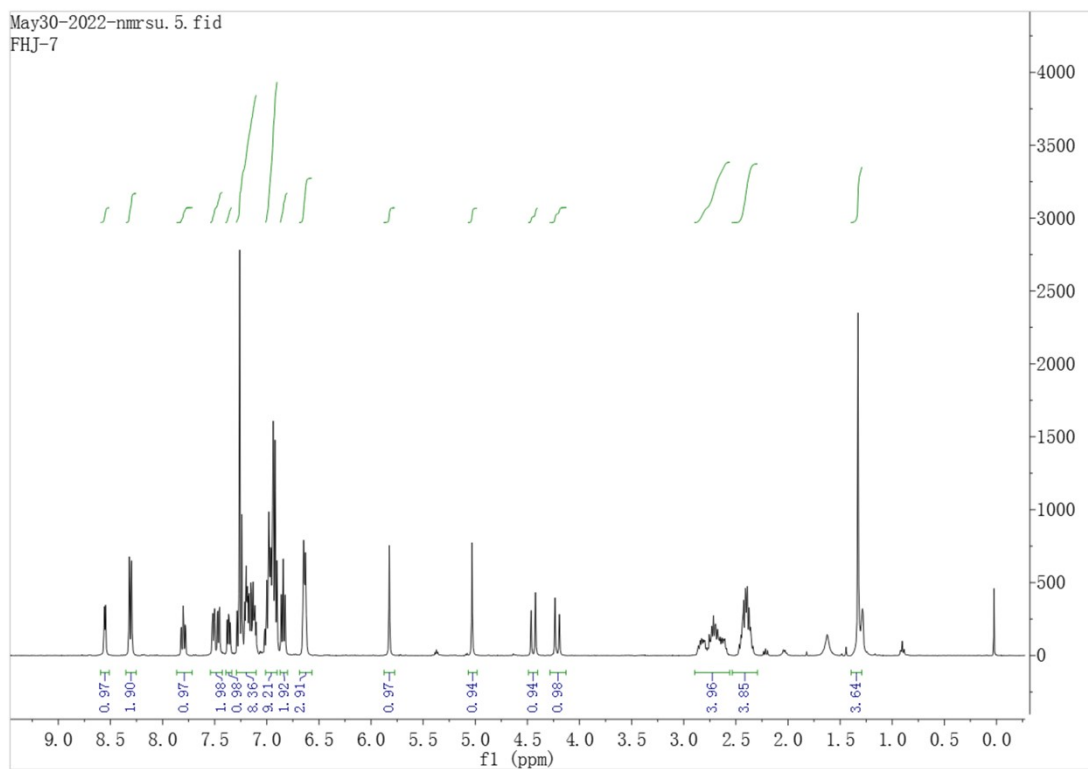


**Figure S7.**  $^1\text{H}$  NMR spectrum of **L3** in  $\text{CDCl}_3$ .

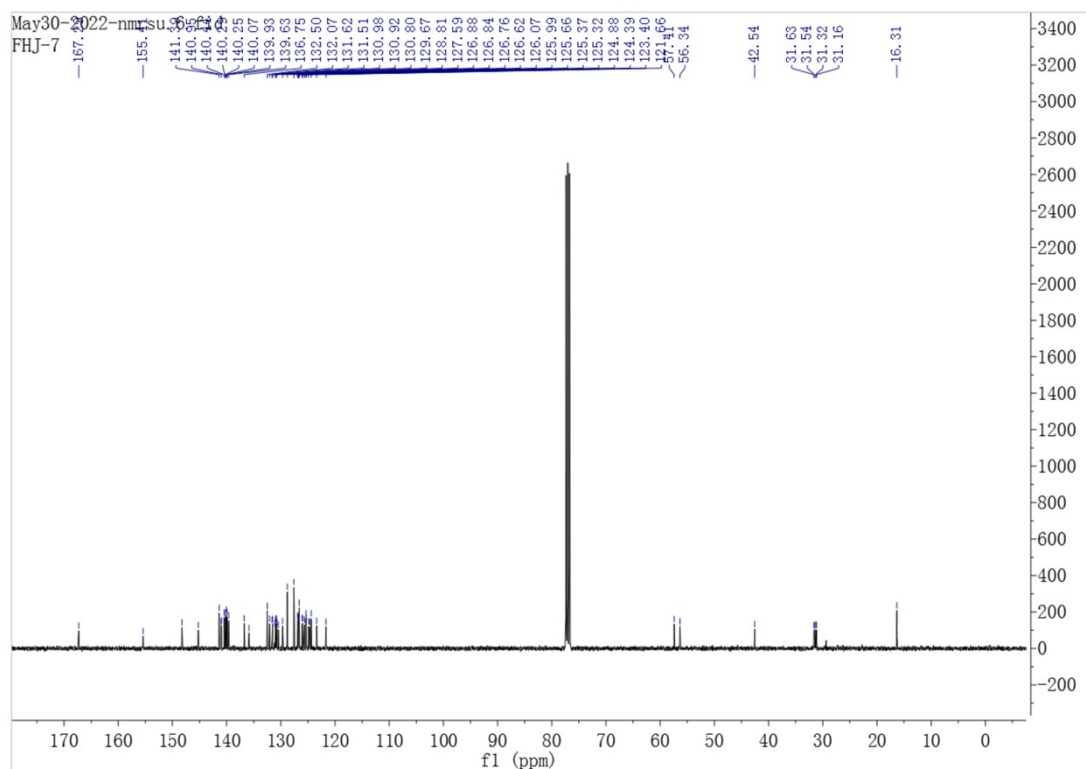


**Figure S8.**  $^{13}\text{C}$  NMR spectrum of **L3** in  $\text{CDCl}_3$ .

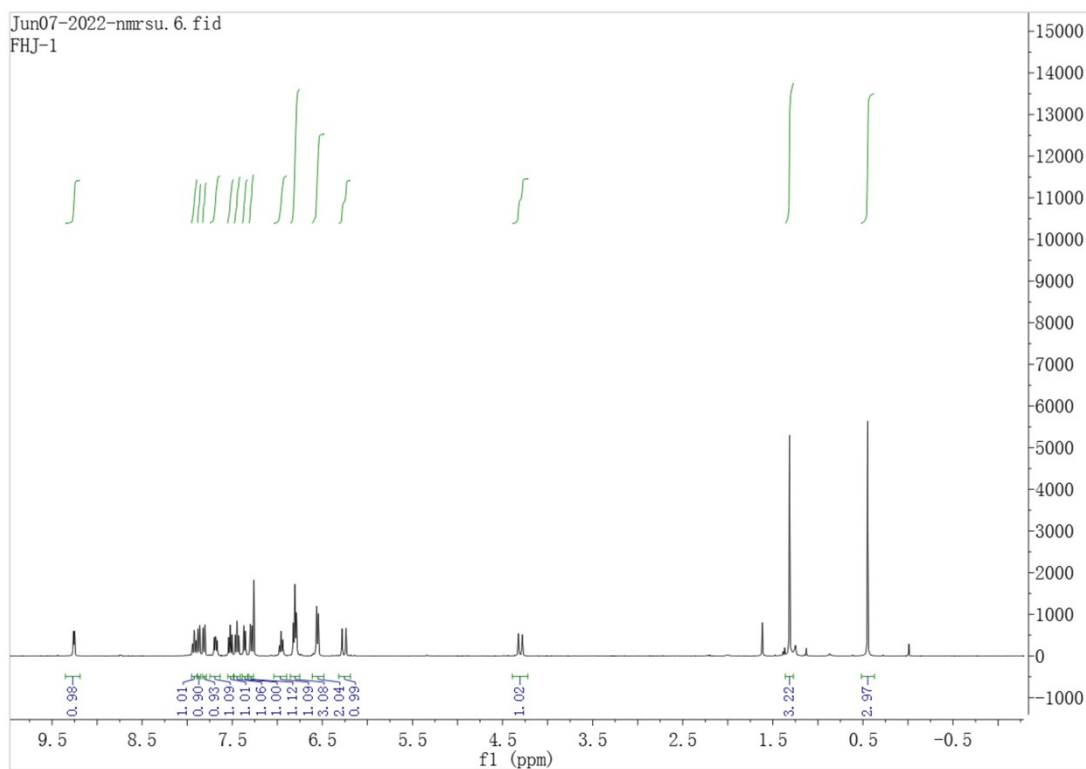


**Figure S9.**  $^1\text{H}$  NMR spectrum of **Pd1** in  $\text{CDCl}_3$ .

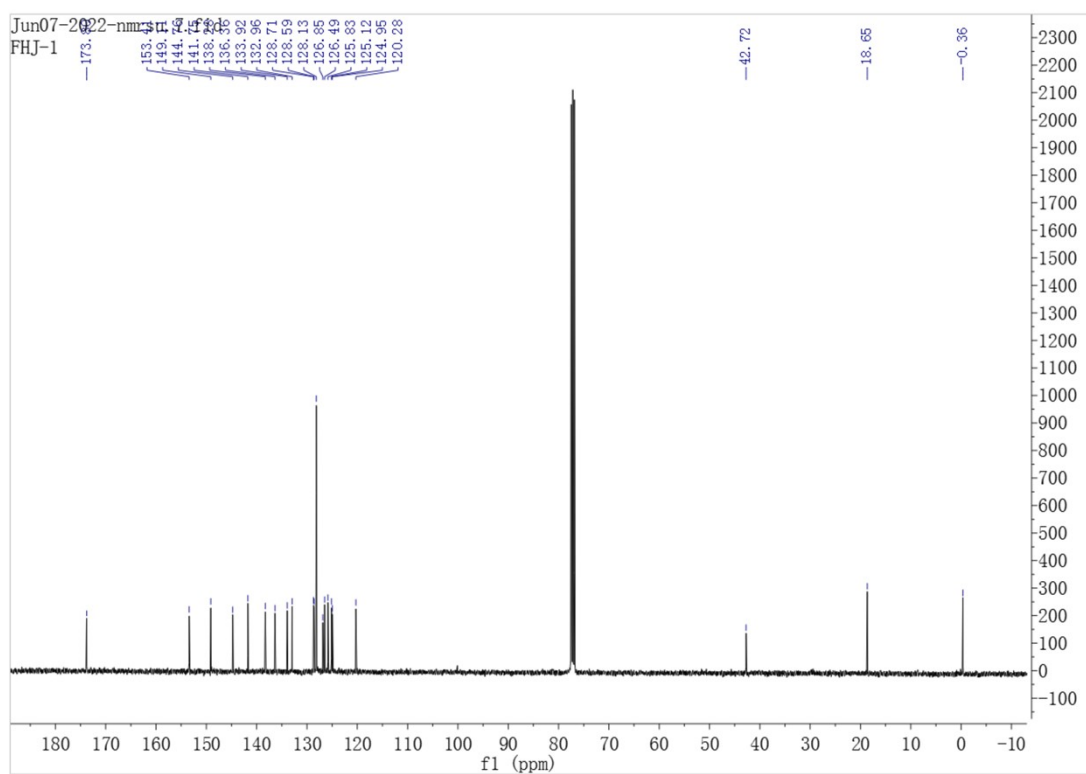


**Figure S10.**  $^{13}\text{C}$  NMR spectrum of **Pd1** in  $\text{CDCl}_3$ .

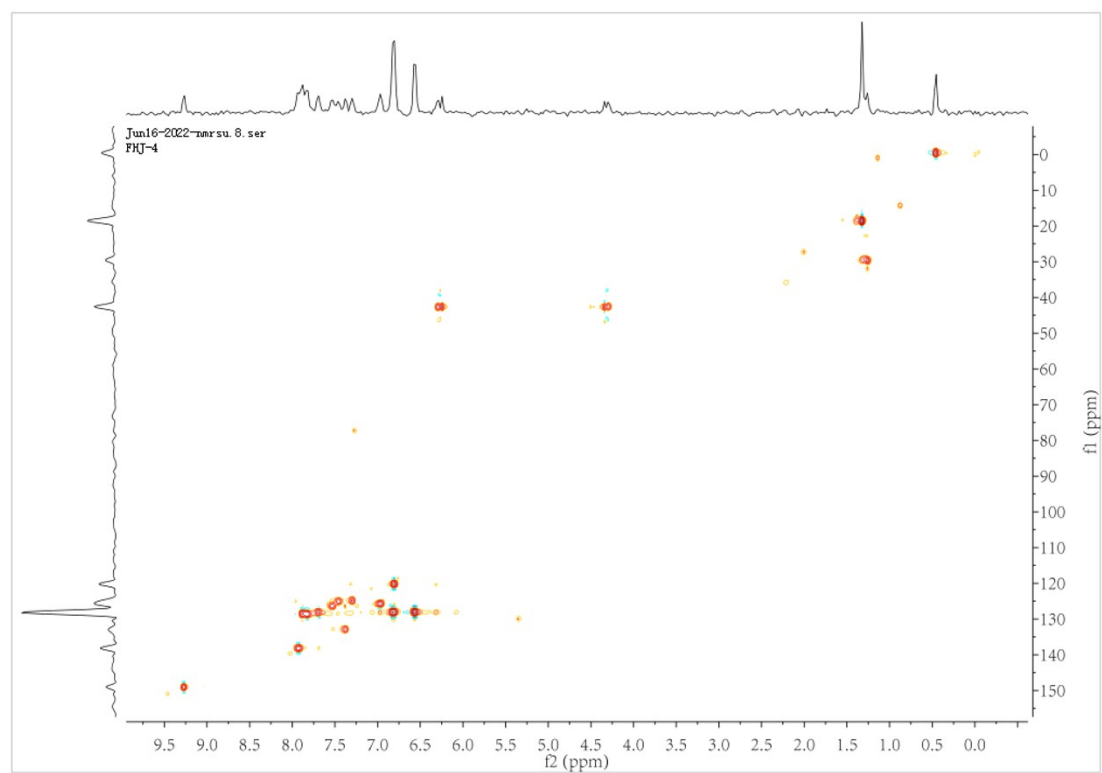


**Figure S11.**  $^1\text{H}$ - $^{13}\text{C}$  HSQC NMR spectrum of **Pd1** in  $\text{CDCl}_3$ .



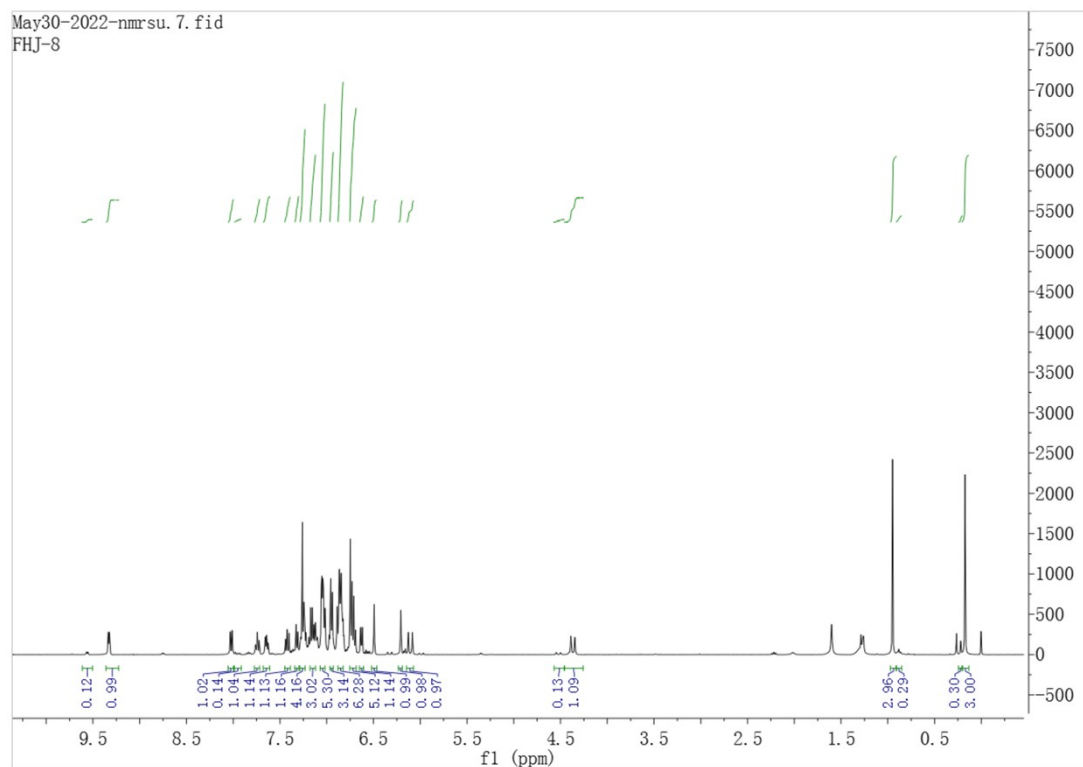


**Figure S12.**  $^1\text{H}$  NMR spectrum of **Pd2** in  $\text{CDCl}_3$ .

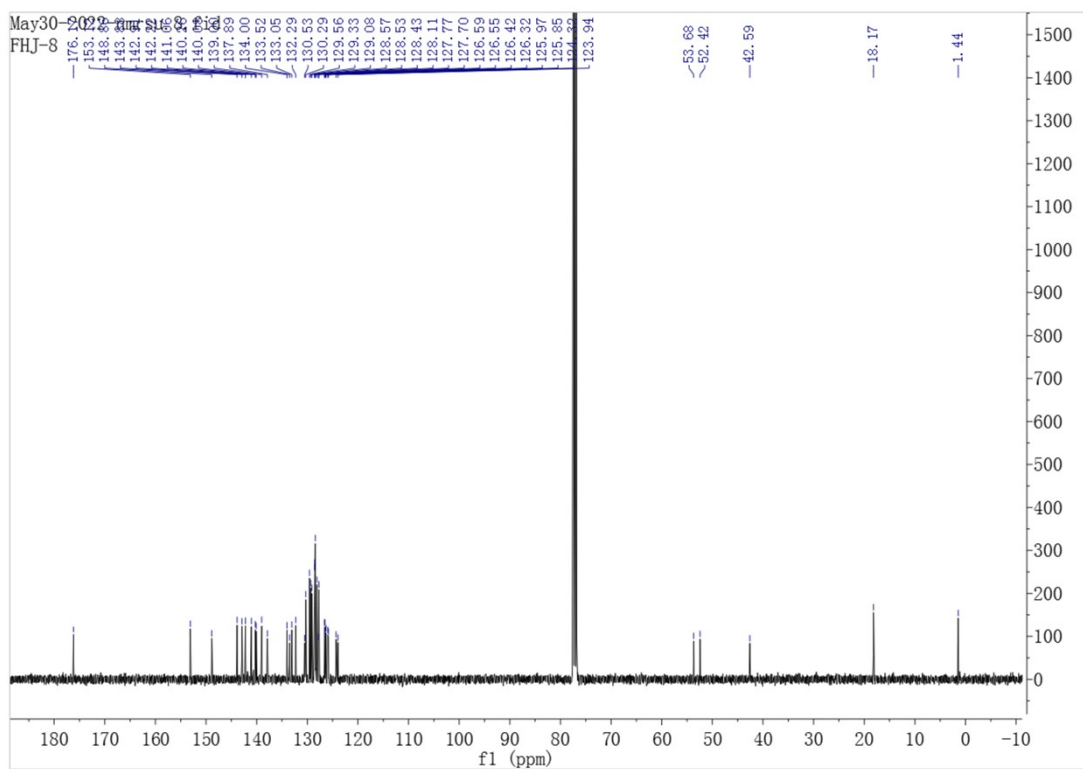


**Figure S13.**  $^{13}\text{C}$  NMR spectrum of **Pd2** in  $\text{CDCl}_3$ .

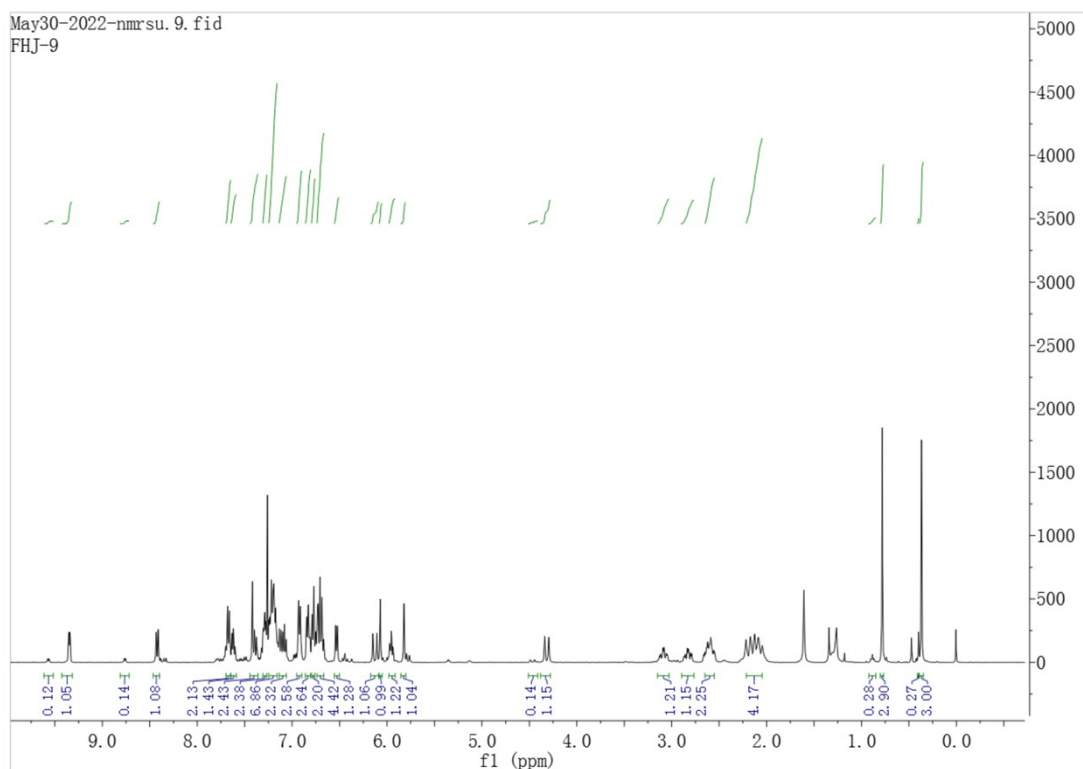


**Figure S14.**  $^1\text{H}$  NMR spectrum of **Pd3** in  $\text{CDCl}_3$ .

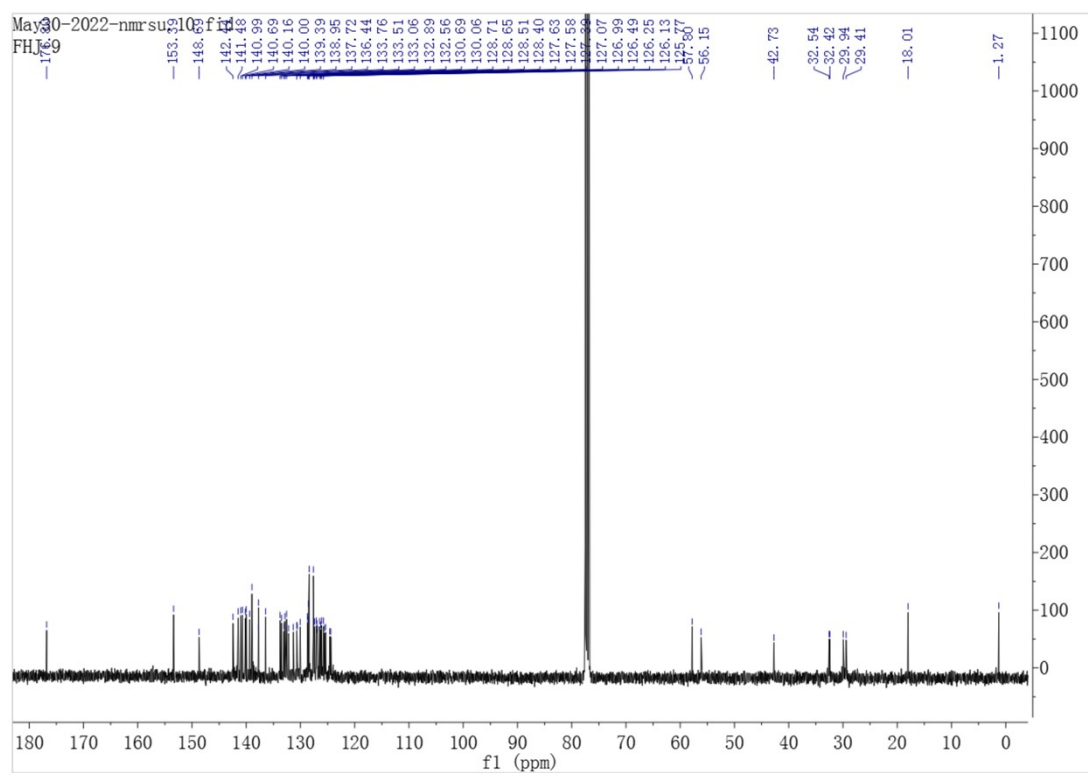


**Figure S15.**  $^{13}\text{C}$  NMR spectrum of **Pd3** in  $\text{CDCl}_3$ .

## 2.2 APCI-MS of Arylamines A2-A3.

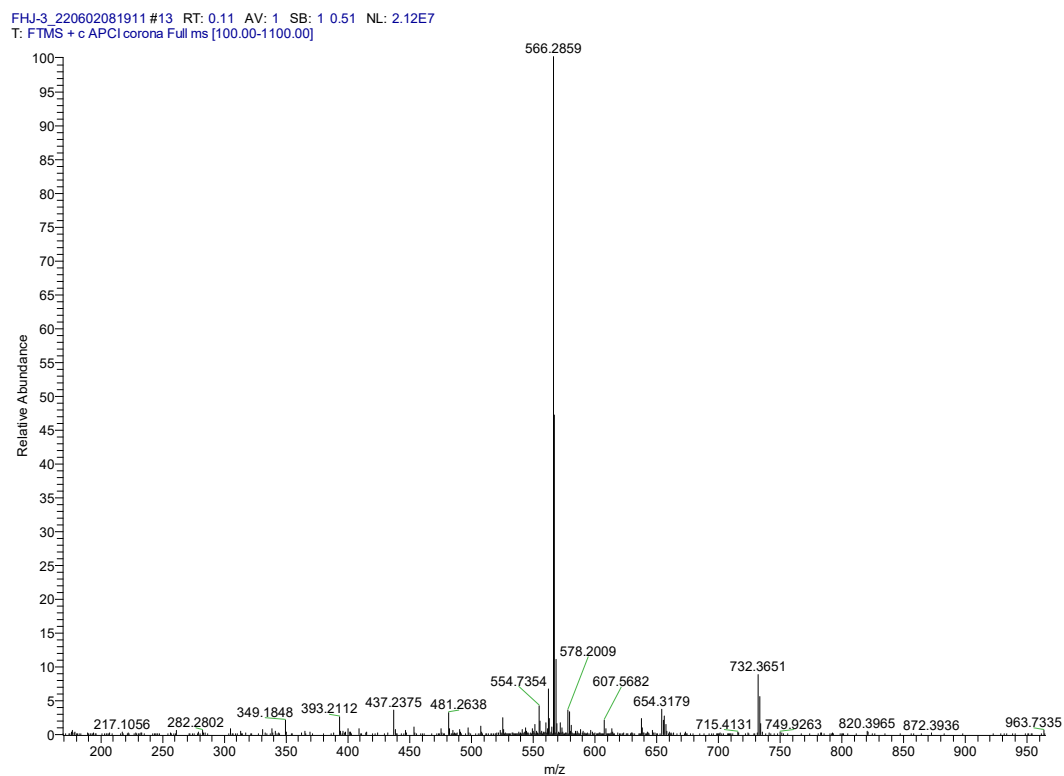


**Figure S16. APCI-MS of A2.**

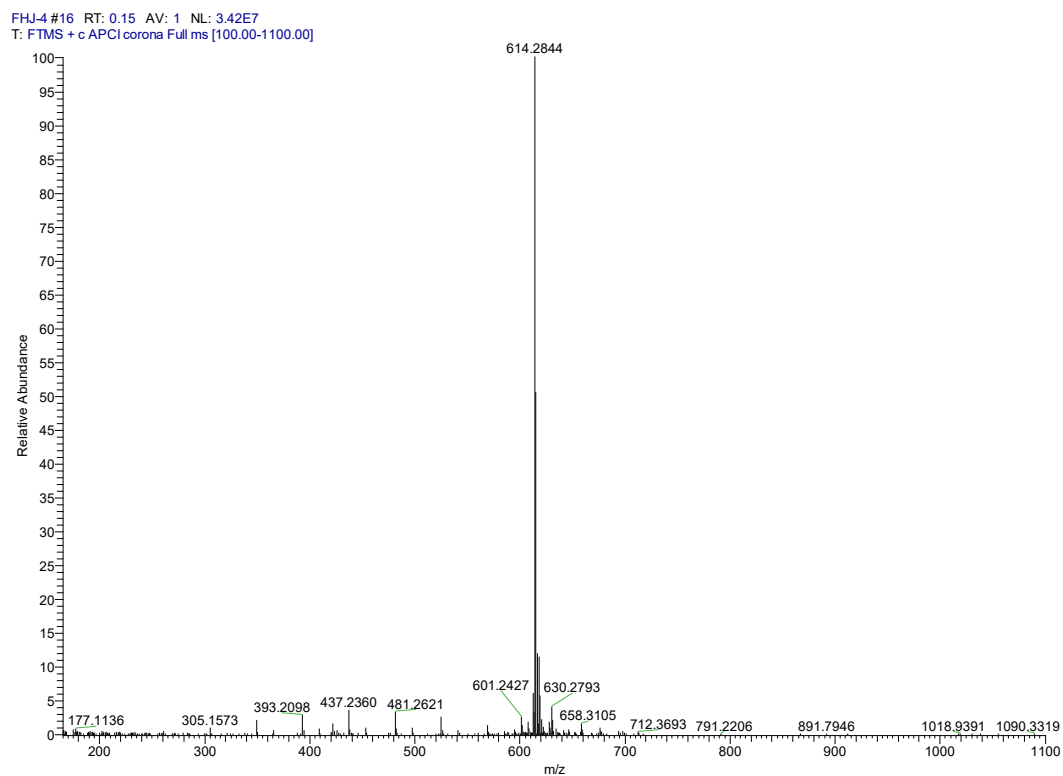


**Figure S17. APCI-MS of A3.**

## 2.3 APCI-MS of Ligands L1-L3.

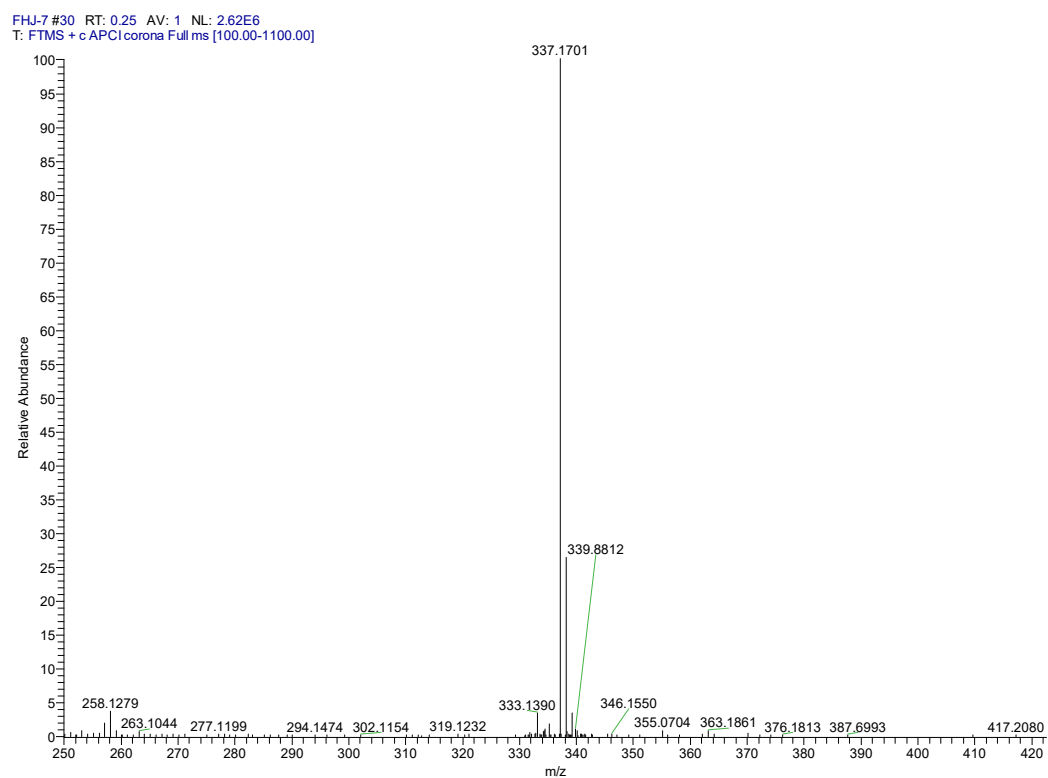


Figure S18. APCI-MS of L1.

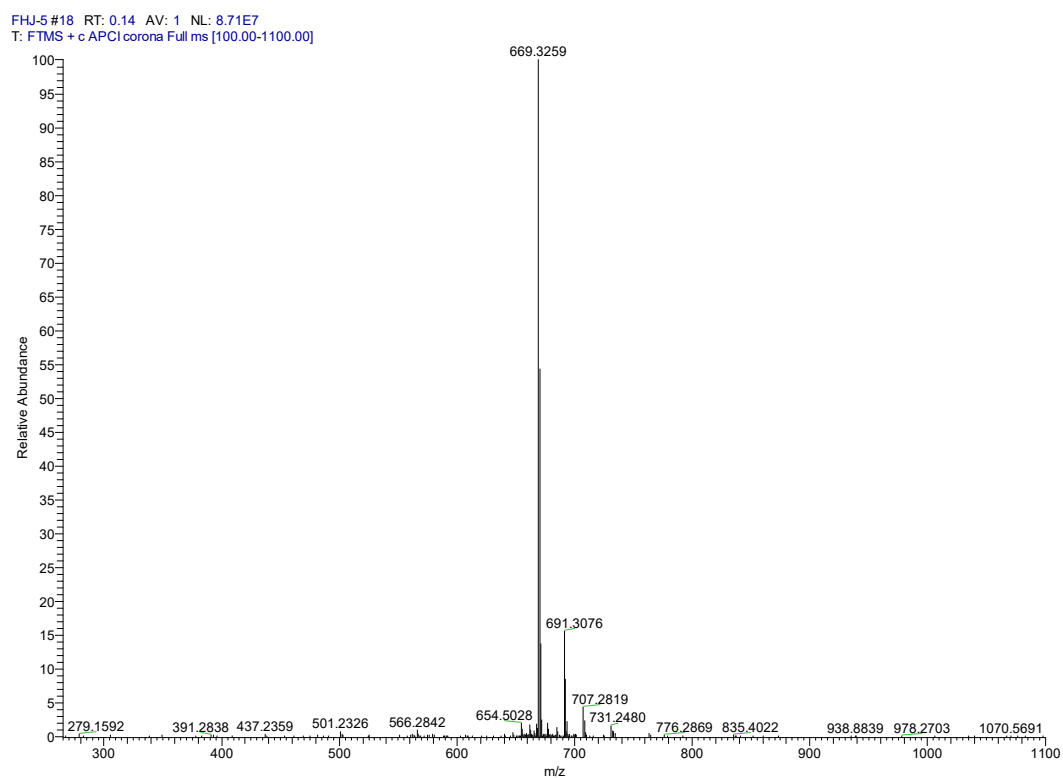
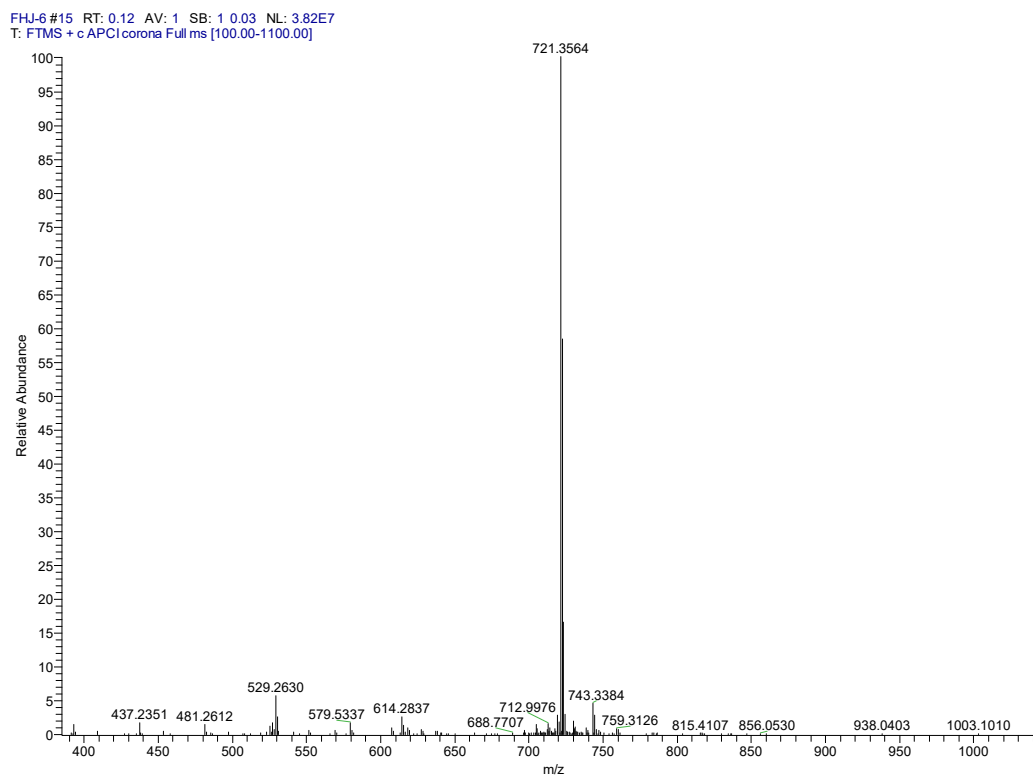
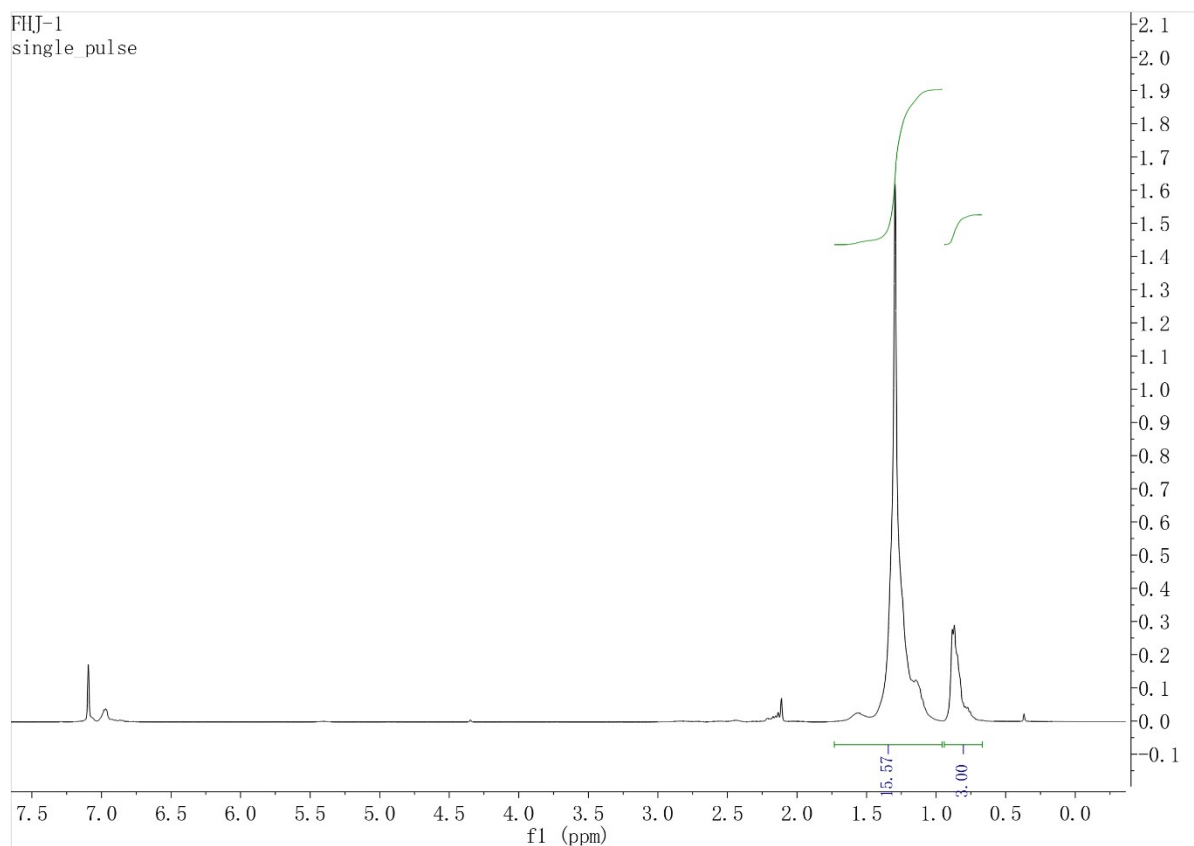


Figure S19. APCI-MS of L2.



**Figure S20.** APCI-MS of L3.

## 2.4 $^1\text{H}$ and $^{13}\text{C}$ NMR of Representative Polymers and Copolymers.



**Figure S21.**  $^1\text{H}$  NMR spectrum of the polymer from table 1, entry 2 ( $\text{C}_6\text{D}_6$ , 70  $^\circ\text{C}$ ).

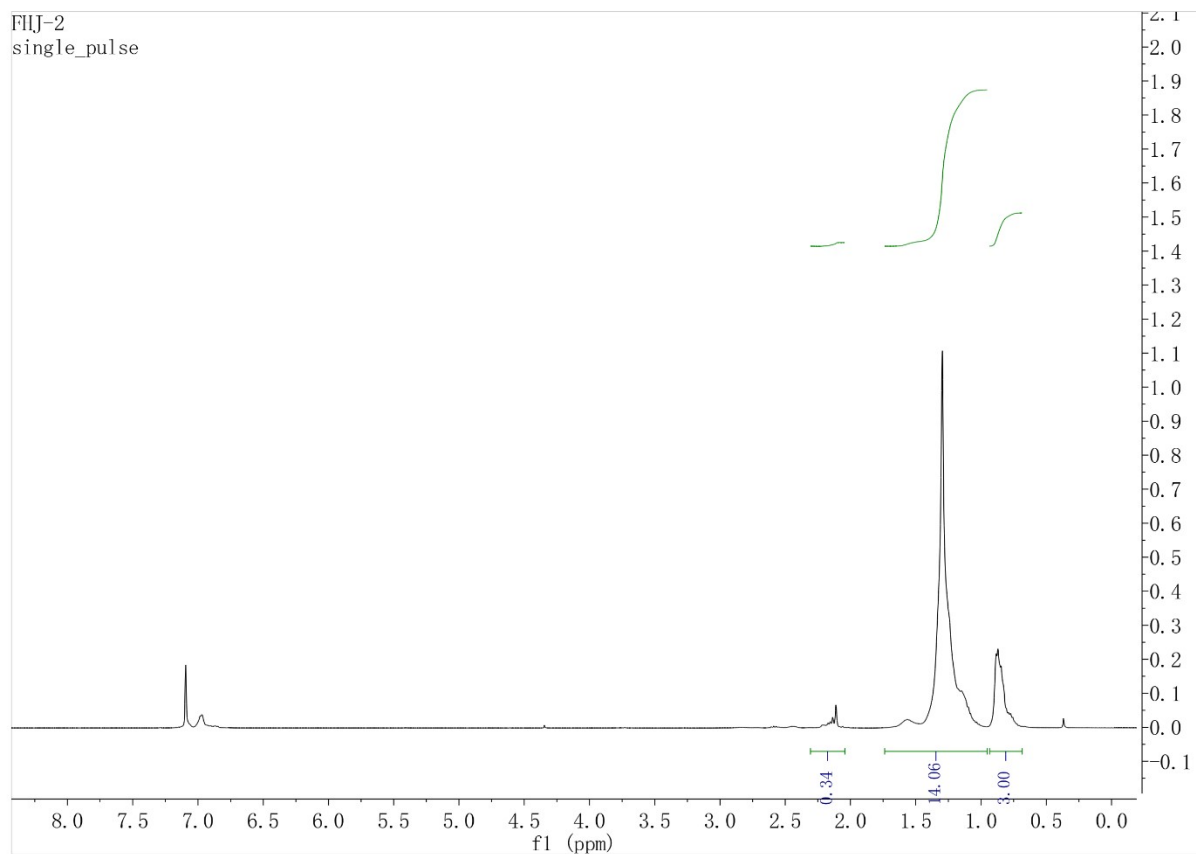


**Figure S22.**  $^1\text{H}$  NMR spectrum of the polymer from table 1, entry 3 ( $\text{C}_6\text{D}_6$ , 70  $^\circ\text{C}$ ).

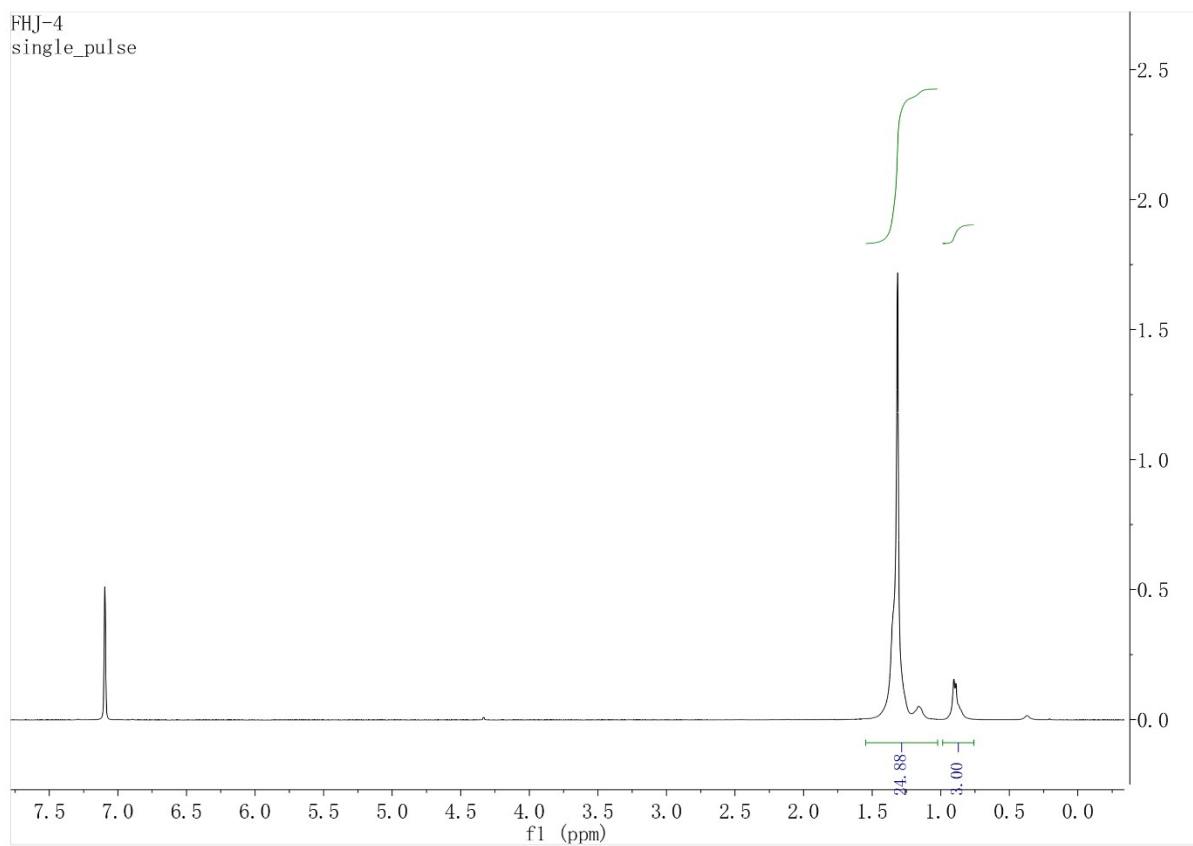


**Figure S23.**  $^1\text{H}$  NMR spectrum of the polymer from table 1, entry 4 ( $\text{C}_6\text{D}_6$ , 70  $^\circ\text{C}$ ).

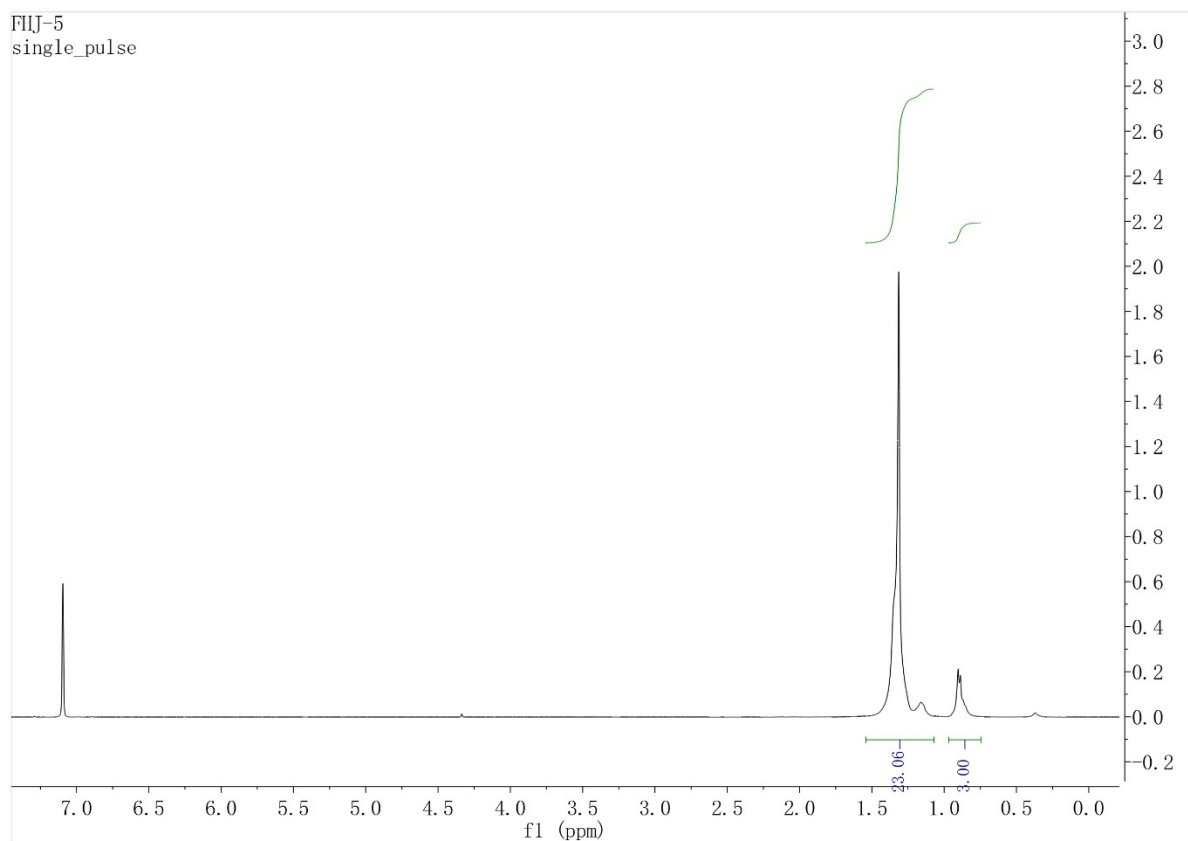


**Figure S24.**  $^1\text{H}$  NMR spectrum of the polymer from table 1, entry 5 ( $\text{C}_6\text{D}_6$ ,  $70^\circ\text{C}$ ).

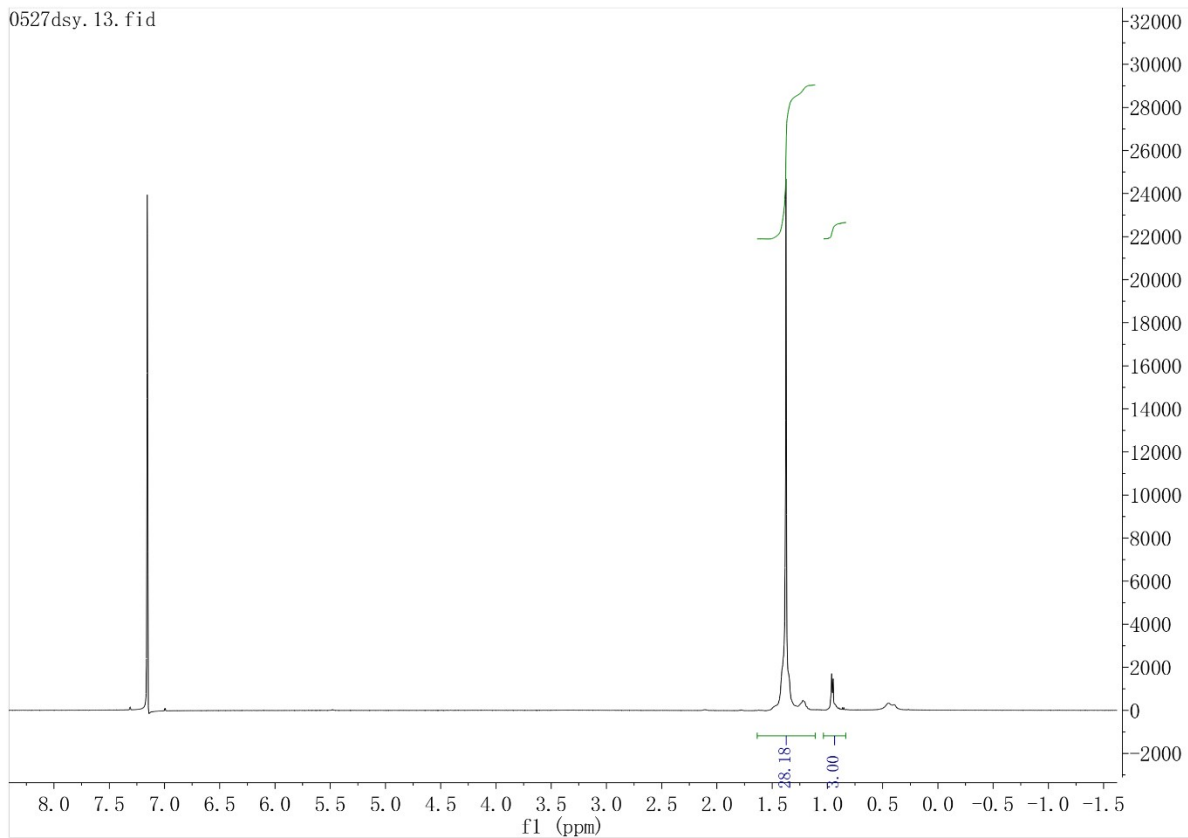


**Figure S25.**  $^1\text{H}$  NMR spectrum of the polymer from table 1, entry 7 ( $\text{C}_6\text{D}_6$ ,  $70^\circ\text{C}$ ).

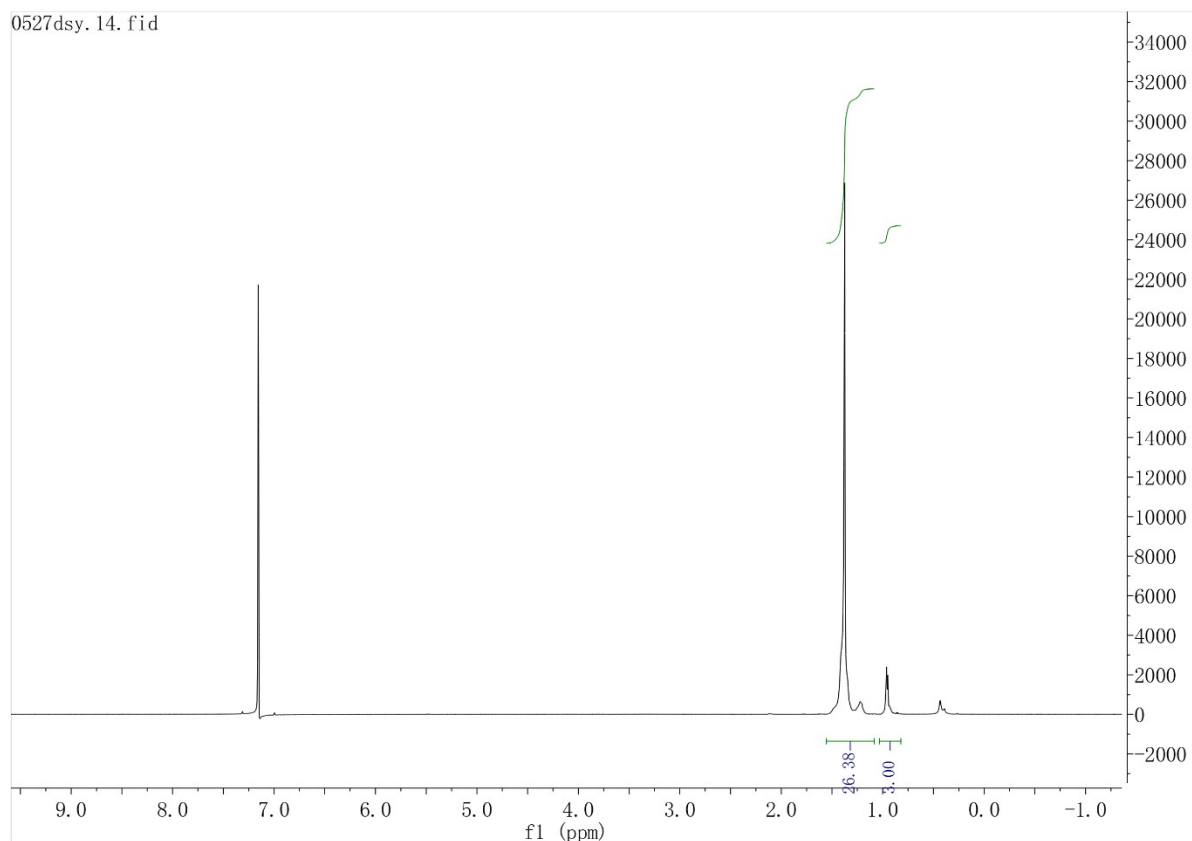


**Figure S26.**  $^1\text{H}$  NMR spectrum of the polymer from table 1, entry 8 ( $\text{C}_6\text{D}_6$ ,  $70^\circ\text{C}$ ).

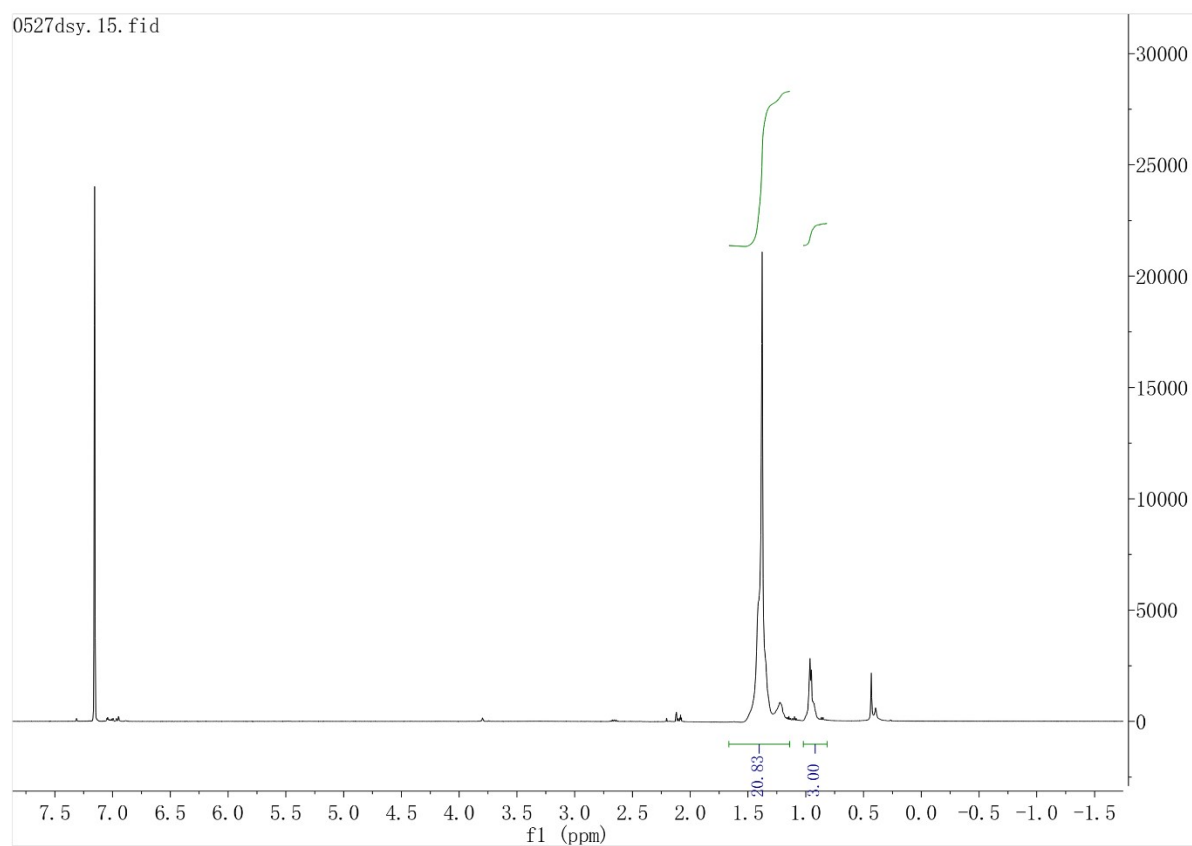


**Figure S27.**  $^1\text{H}$  NMR spectrum of the polymer from table 1, entry 9 ( $\text{C}_6\text{D}_6$ ,  $70^\circ\text{C}$ ).



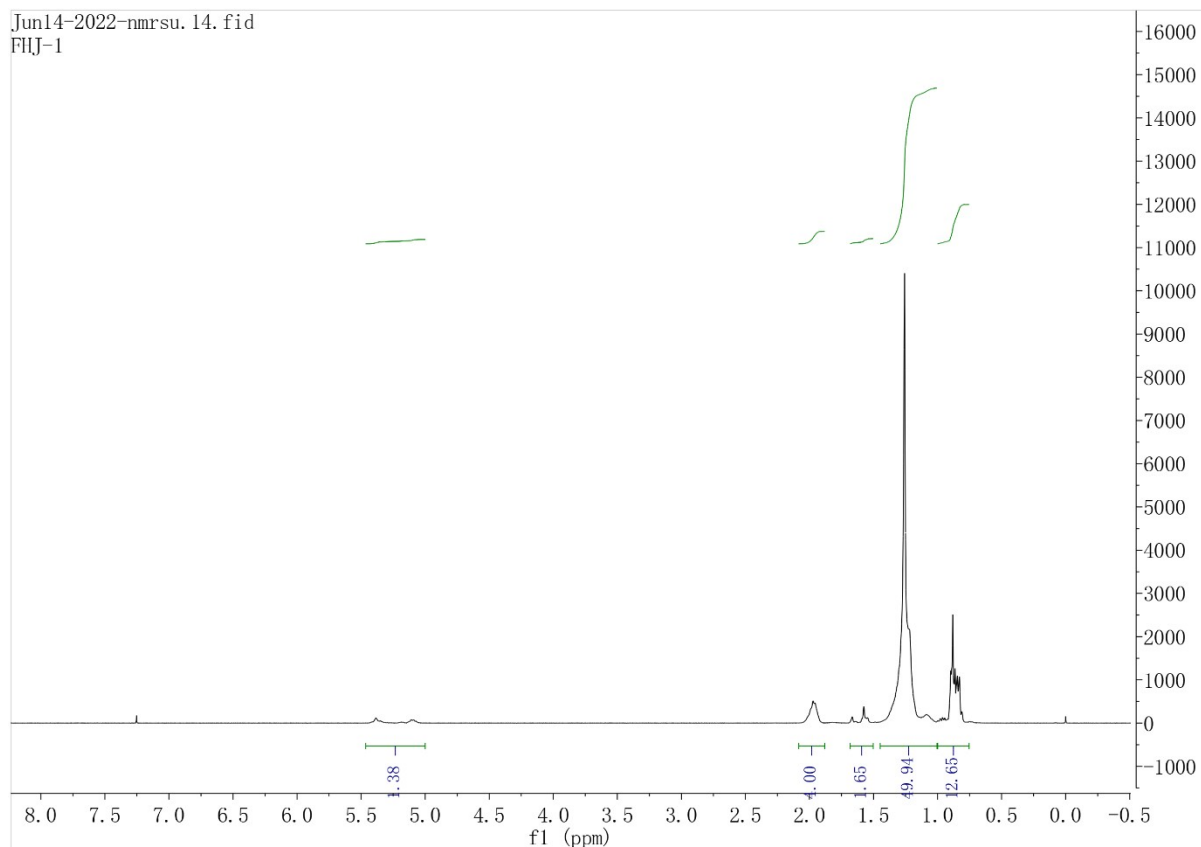


**Figure S28.**  $^1\text{H}$  NMR spectrum of the polymer from table 2, entry 1 ( $\text{CDCl}_3$ , 20  $^\circ\text{C}$ ).

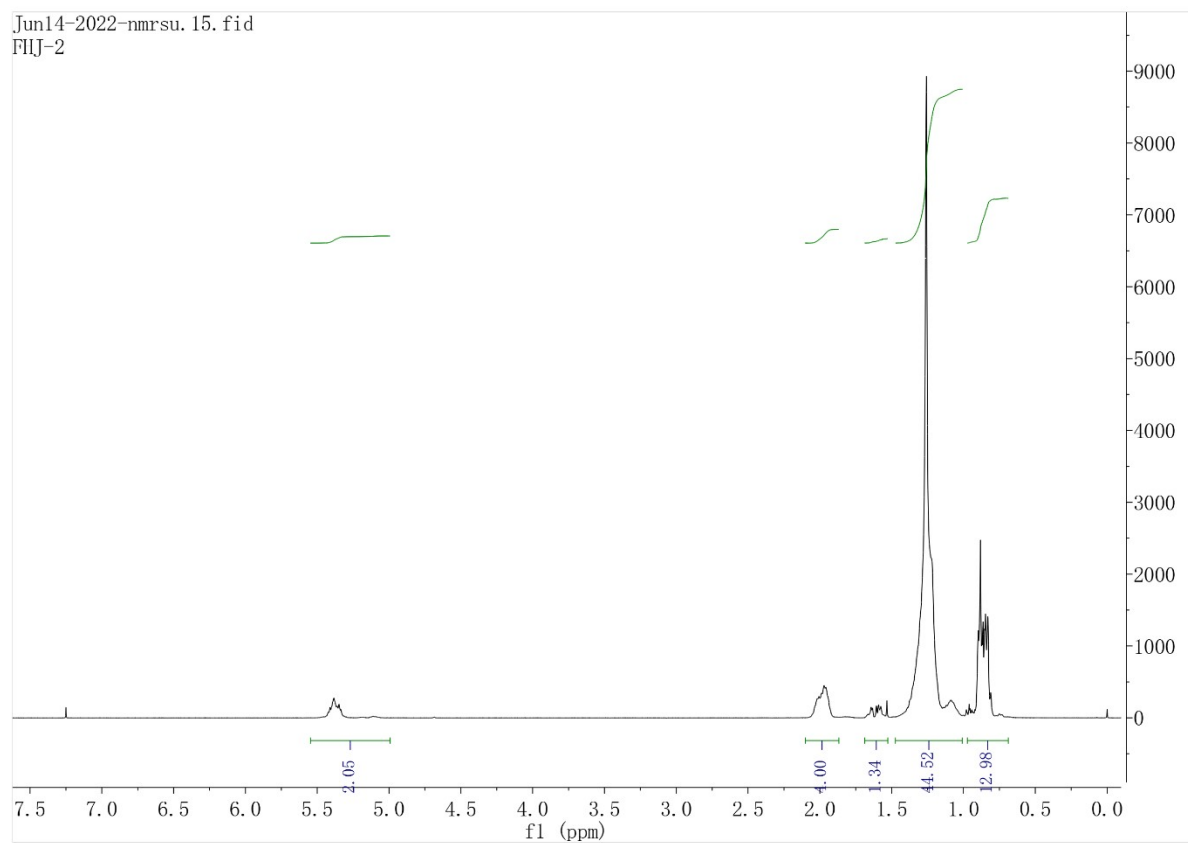


**Figure S29.**  $^1\text{H}$  NMR spectrum of the polymer from table 2, entry 2 ( $\text{CDCl}_3$ , 20  $^\circ\text{C}$ ).

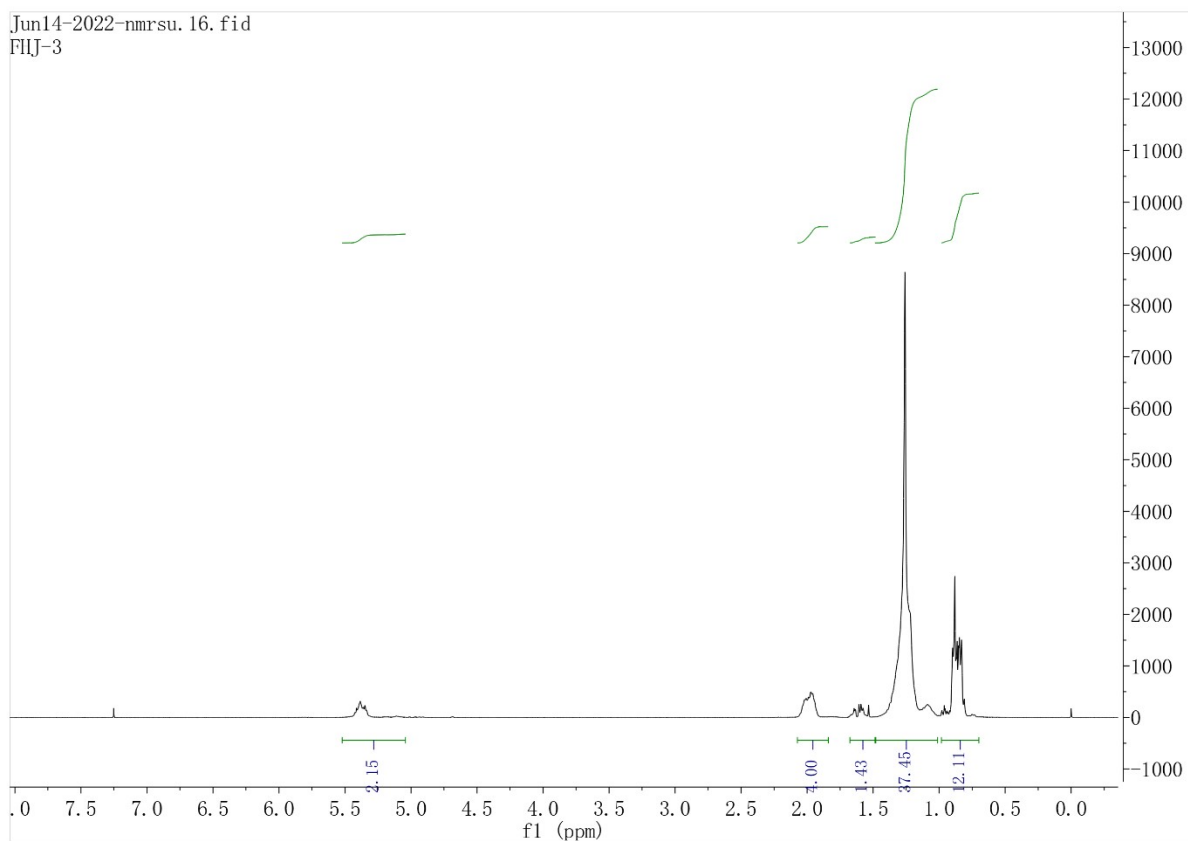


**Figure S30.**  $^1\text{H}$  NMR spectrum of the polymer from table 2, entry 3 ( $\text{CDCl}_3$ , 20  $^\circ\text{C}$ ).

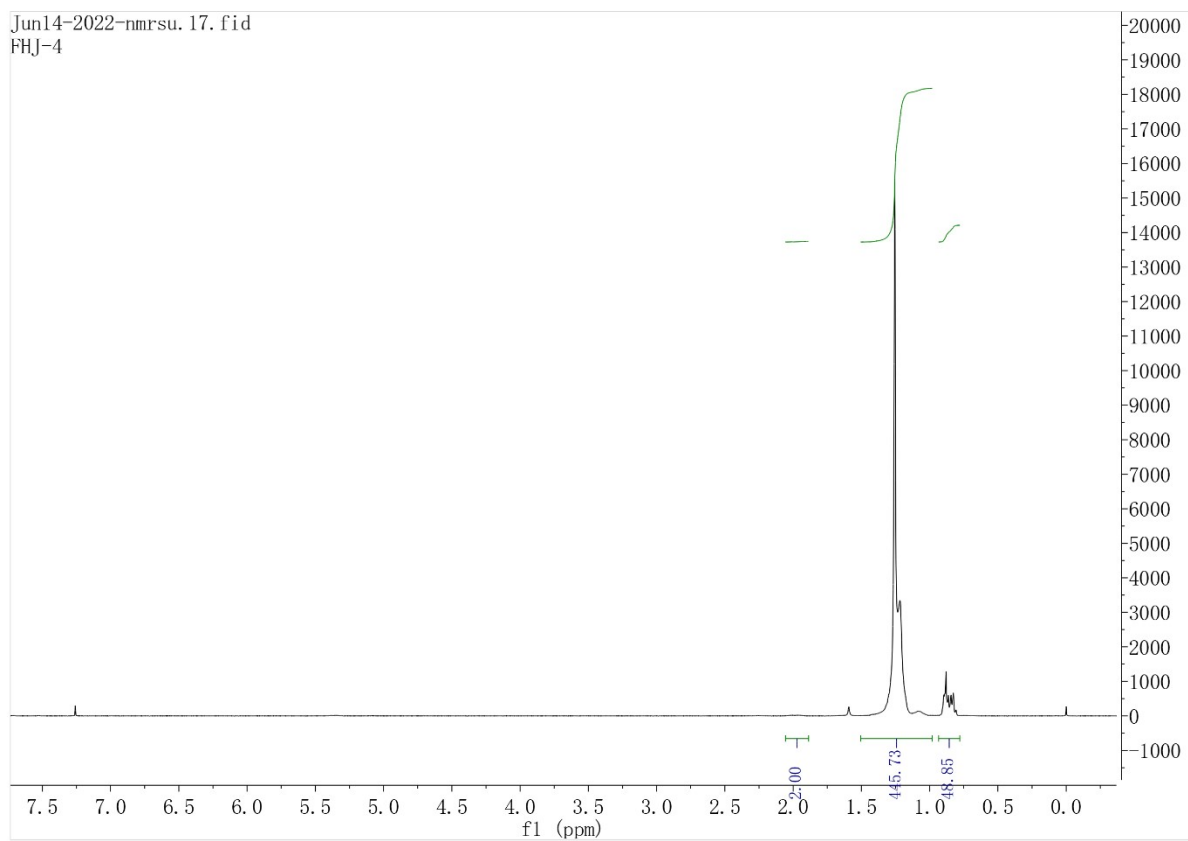


**Figure S31.**  $^1\text{H}$  NMR spectrum of the polymer from table 2, entry 4 ( $\text{CDCl}_3$ , 20  $^\circ\text{C}$ ).

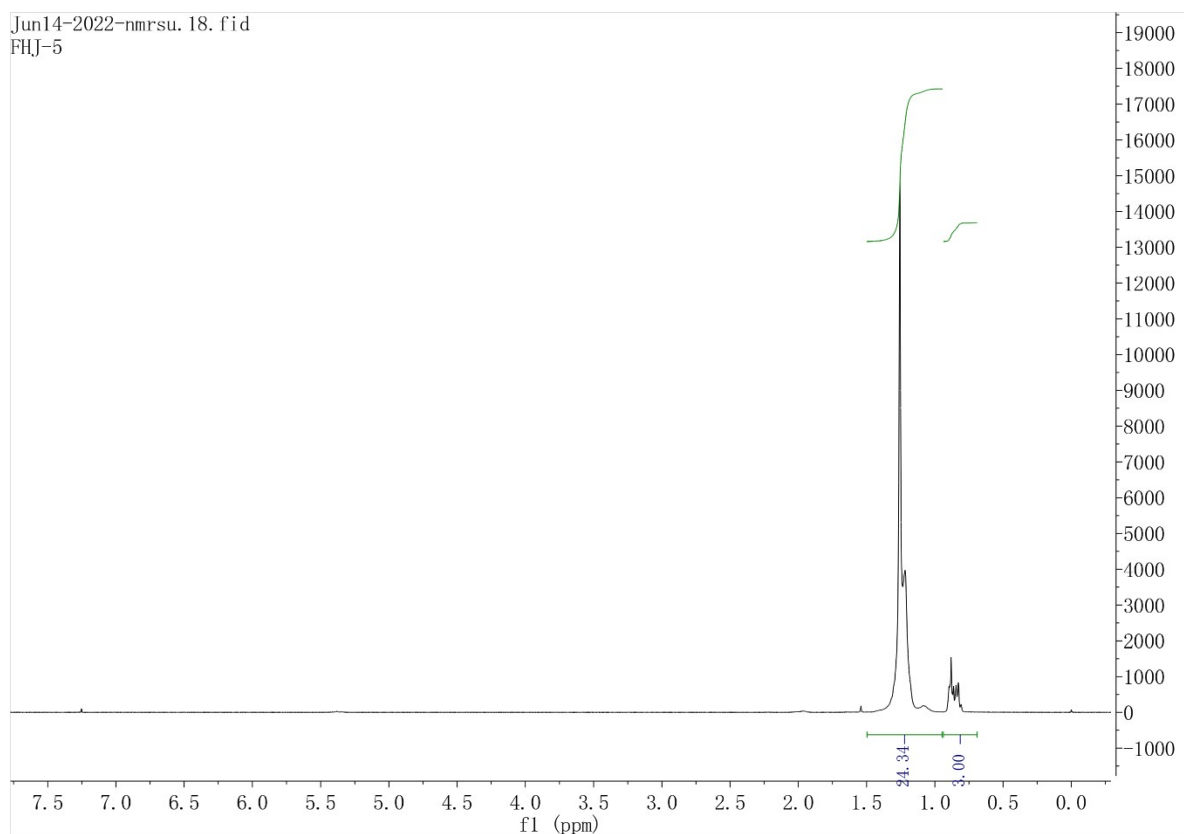


**Figure S32.**  $^1\text{H}$  NMR spectrum of the polymer from table 2, entry 5 ( $\text{CDCl}_3$ , 20  $^\circ\text{C}$ ).

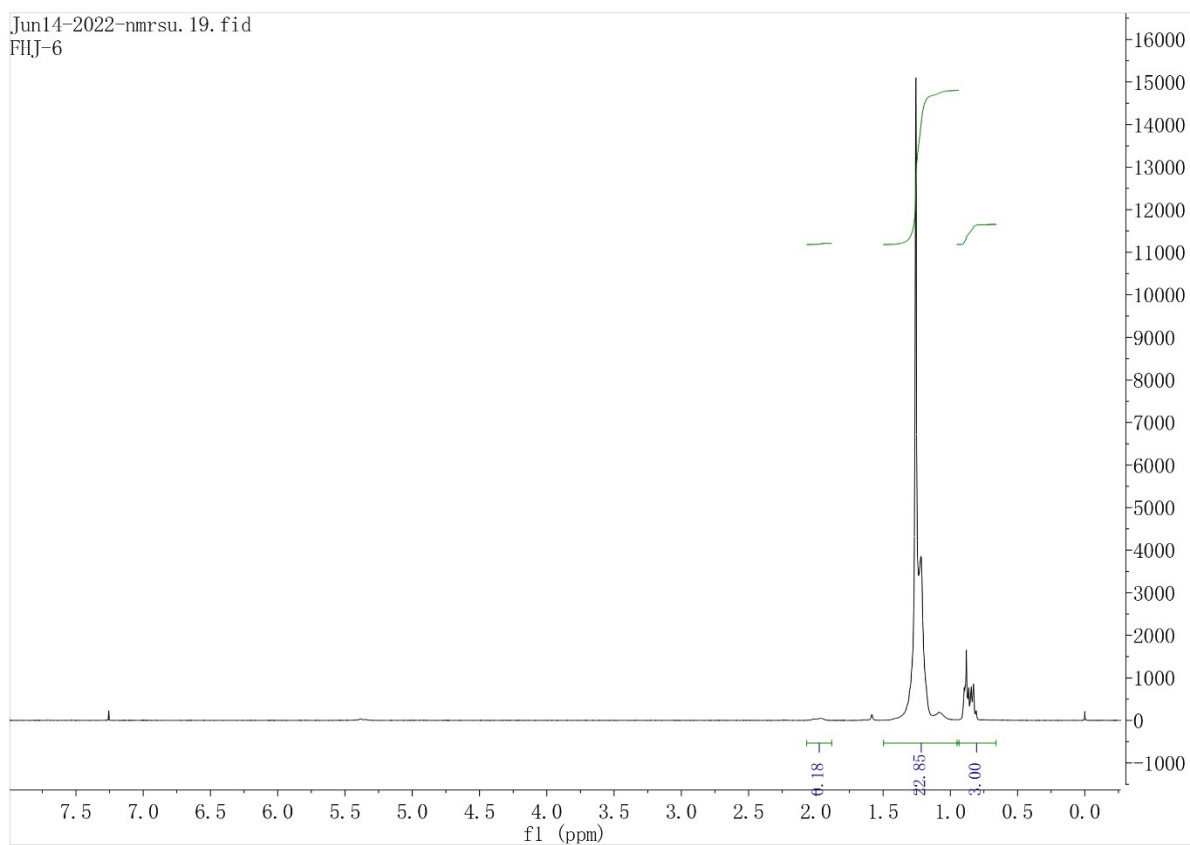


**Figure S33.**  $^1\text{H}$  NMR spectrum of the polymer from table 2, entry 6 ( $\text{CDCl}_3$ , 20  $^\circ\text{C}$ ).

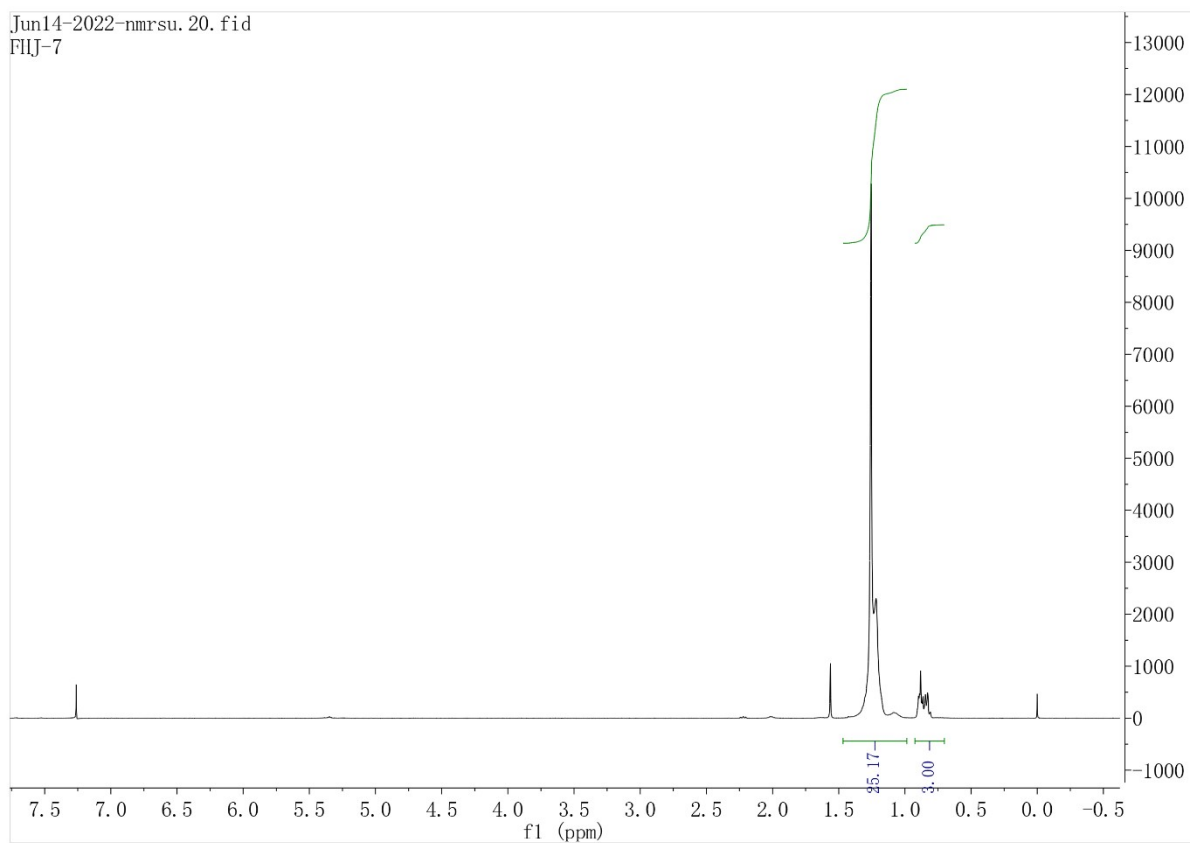


**Figure S34.**  $^1\text{H}$  NMR spectrum of the polymer from table 2, entry 7 ( $\text{CDCl}_3$ , 20  $^\circ\text{C}$ ).

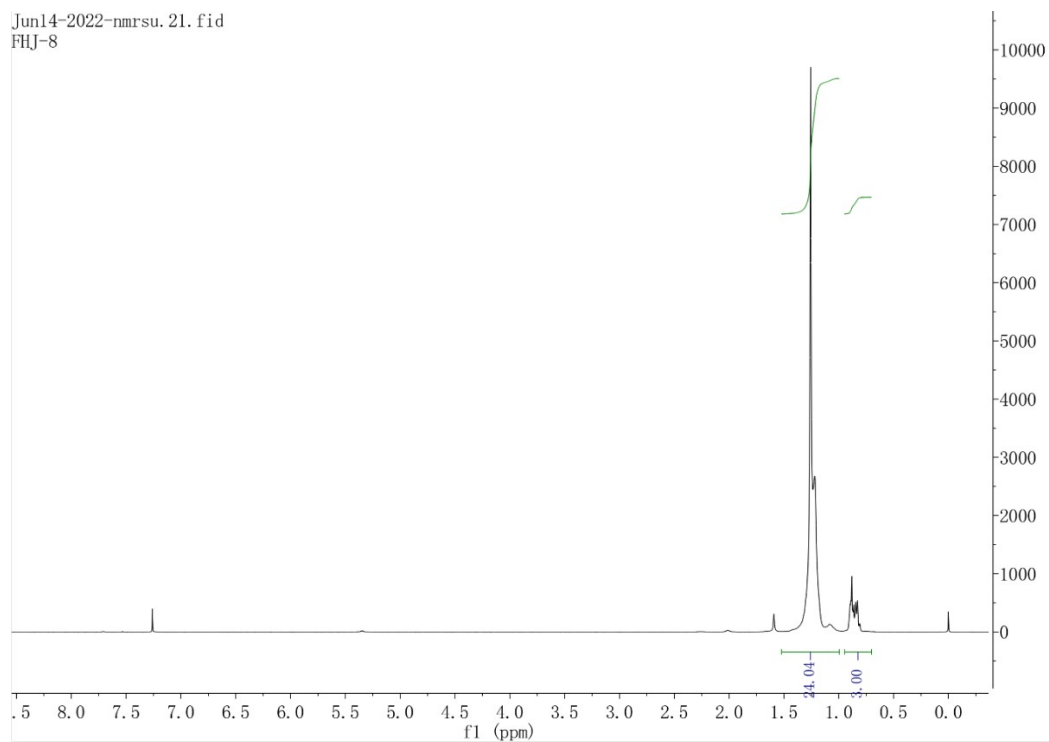


**Figure S35.**  $^1\text{H}$  NMR spectrum of the polymer from table 2, entry 8 ( $\text{CDCl}_3$ , 20  $^\circ\text{C}$ ).

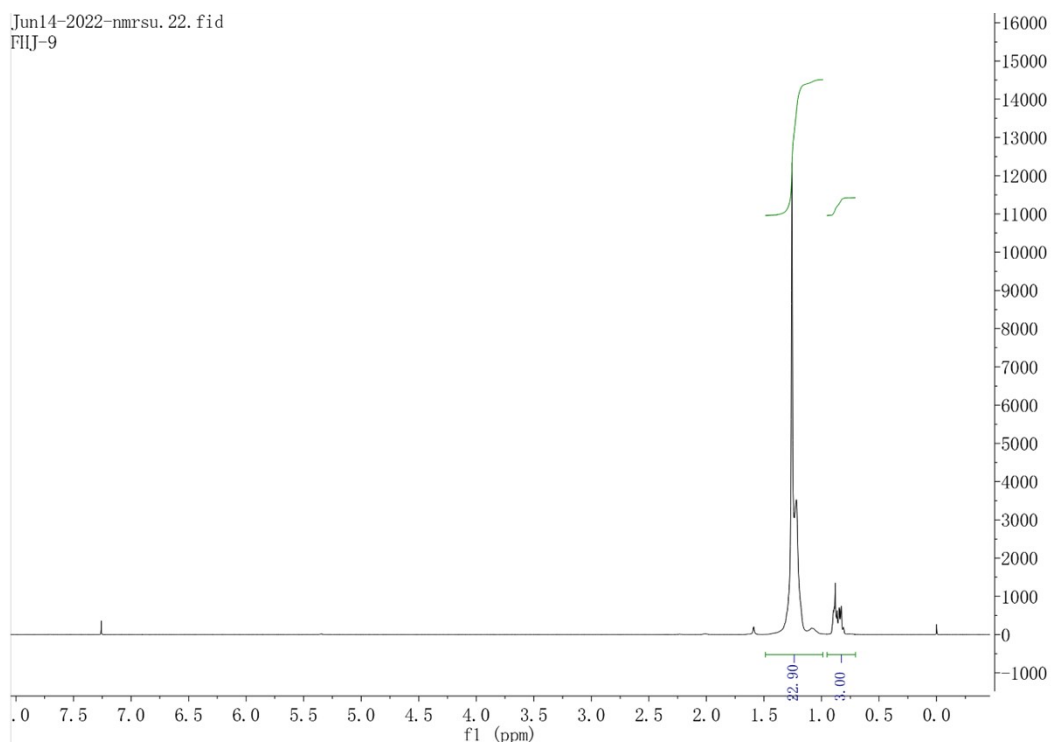


**Figure S36.**  $^1\text{H}$  NMR spectrum of the polymer from table 2, entry 9 ( $\text{CDCl}_3$ ,  $20^\circ\text{C}$ ).

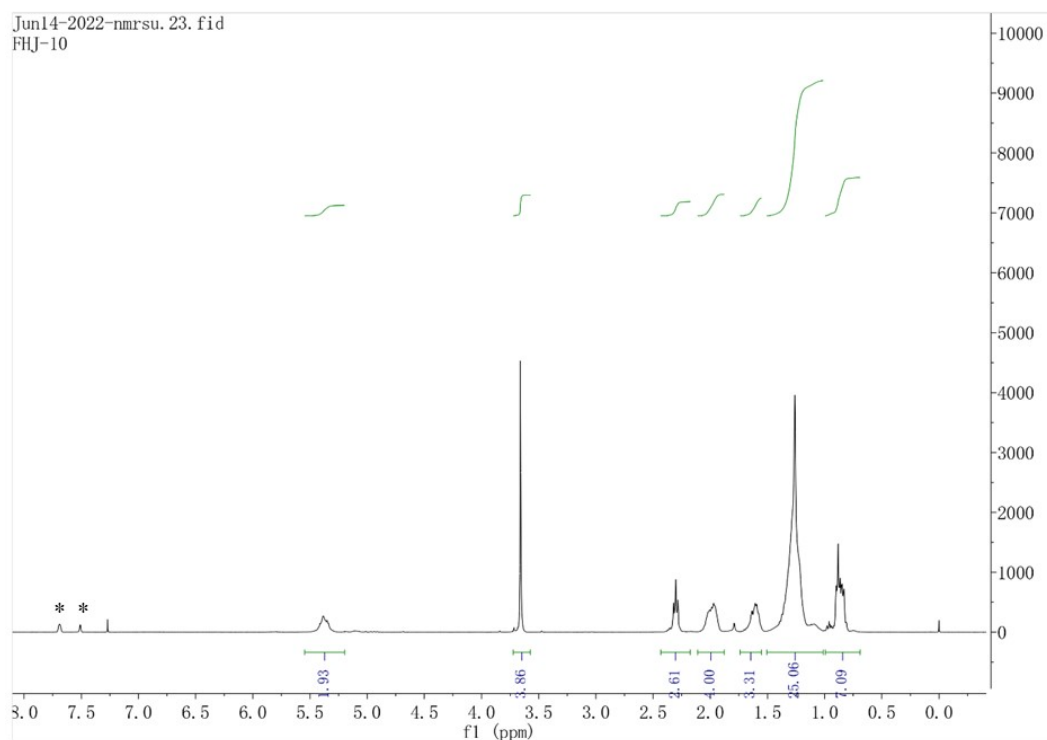


**Figure S37.**  $^1\text{H}$  NMR spectrum of the copolymer from table 3, entry 1 ( $\text{CDCl}_3$ ,  $20^\circ\text{C}$ ). \* H of  $\text{BArF}^-$  anion (tetrakis(3,5-bis(trifluoromethyl)phenyl)borate).

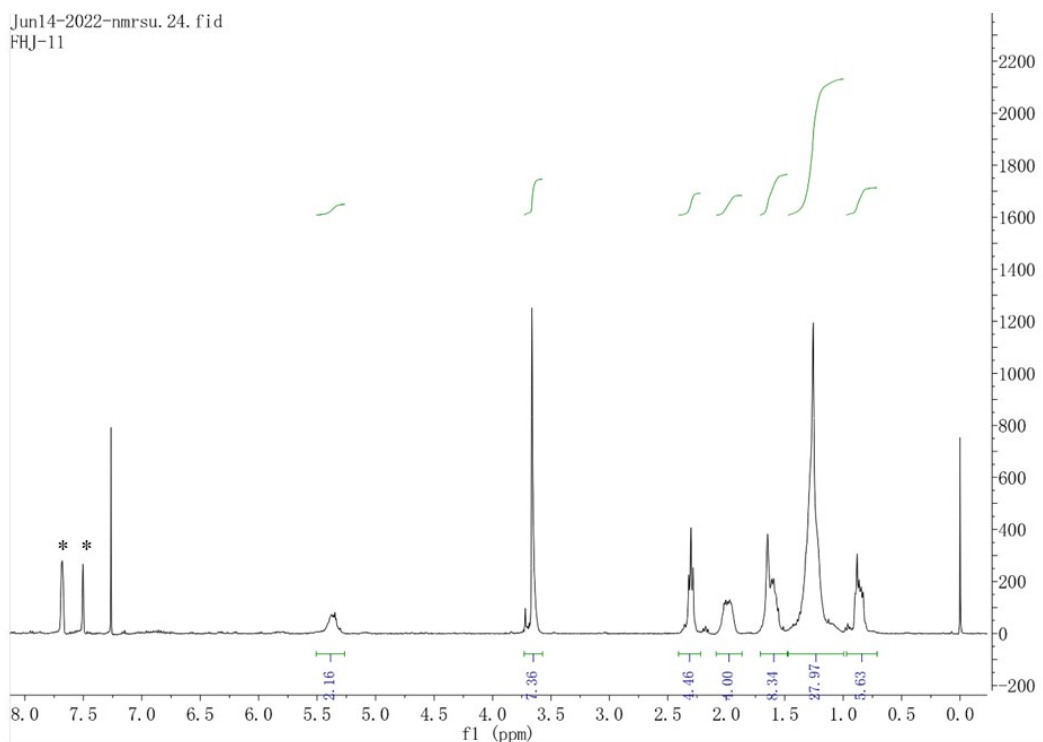


**Figure S38.**  $^1\text{H}$  NMR spectrum of the copolymer from table 3, entry 2 ( $\text{CDCl}_3$ , 20  $^\circ\text{C}$ ). \* H of  $\text{BArF}^-$  anion (tetrakis(3,5-bis(trifluoromethyl)phenyl)borate).

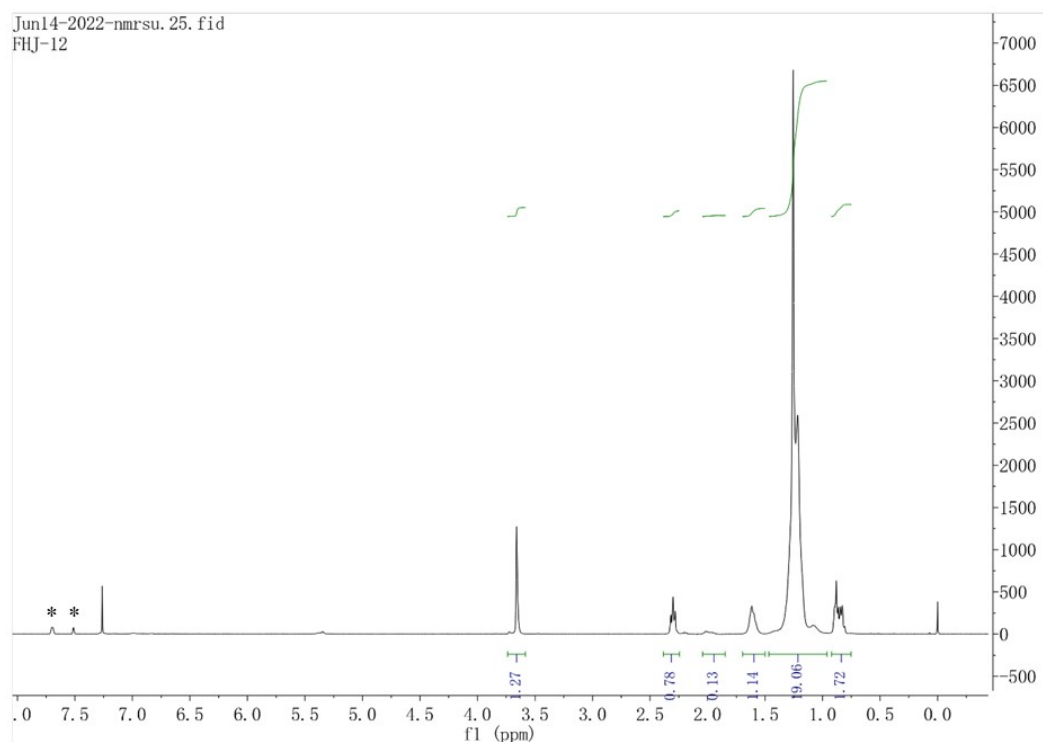


**Figure S39.**  $^1\text{H}$  NMR spectrum of the copolymer from table 3, entry 3 ( $\text{CDCl}_3$ , 20  $^\circ\text{C}$ ). \* H of  $\text{BArF}^-$  anion (tetrakis(3,5-bis(trifluoromethyl)phenyl)borate).

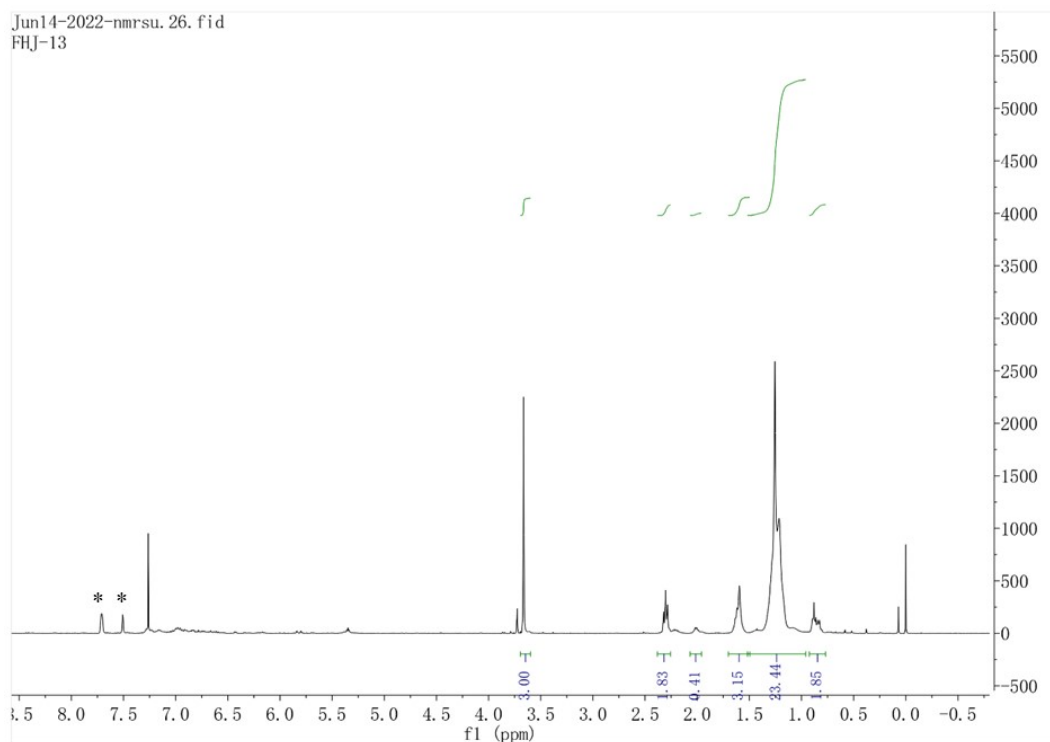


**Figure S40.**  $^1\text{H}$  NMR spectrum of the copolymer from table 3, entry 4 ( $\text{CDCl}_3$ , 20  $^\circ\text{C}$ ). \* H of  $\text{BArF}^-$  anion (tetrakis(3,5-bis(trifluoromethyl)phenyl)borate).

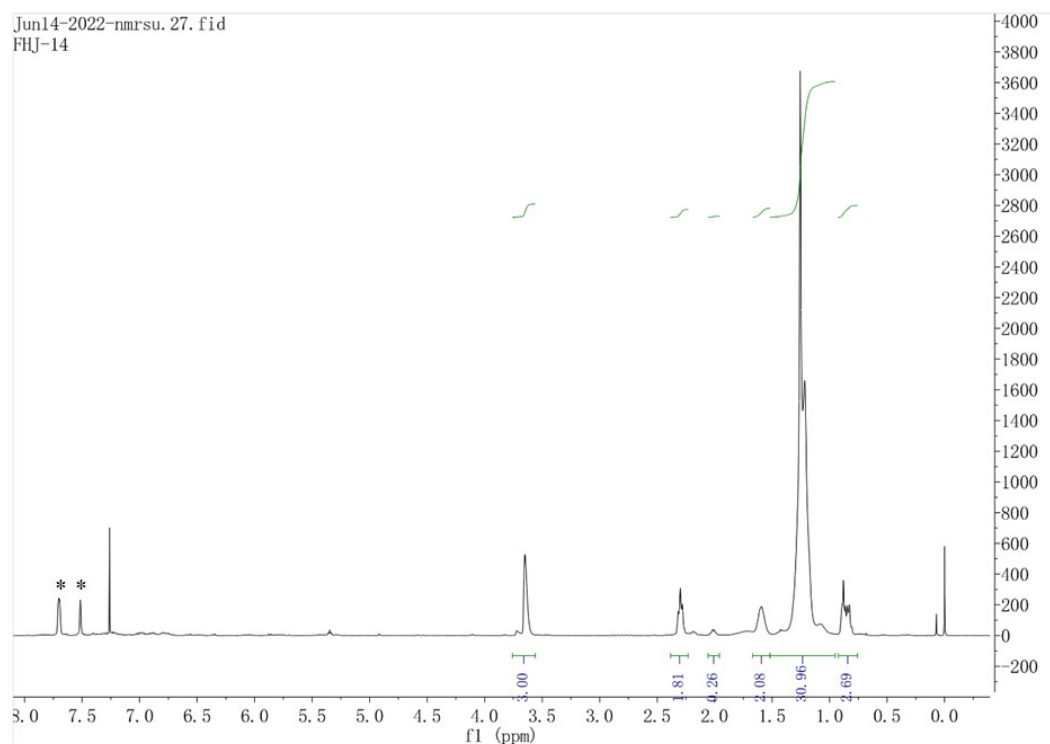


**Figure S41.**  $^1\text{H}$  NMR spectrum of the copolymer from table 3, entry 5 ( $\text{CDCl}_3$ , 20  $^\circ\text{C}$ ). \* H of  $\text{BArF}^-$  anion (tetrakis(3,5-bis(trifluoromethyl)phenyl)borate).

## 2.5 DSC and GPC of Representative Polymers and Copolymers.

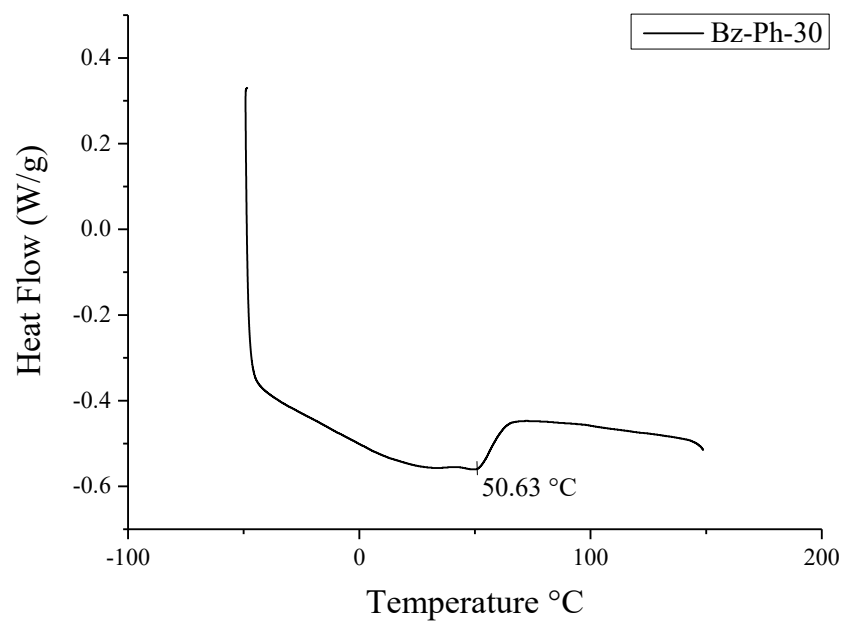


**Figure S42.** DSC of the polymer from table 1, entry 4.

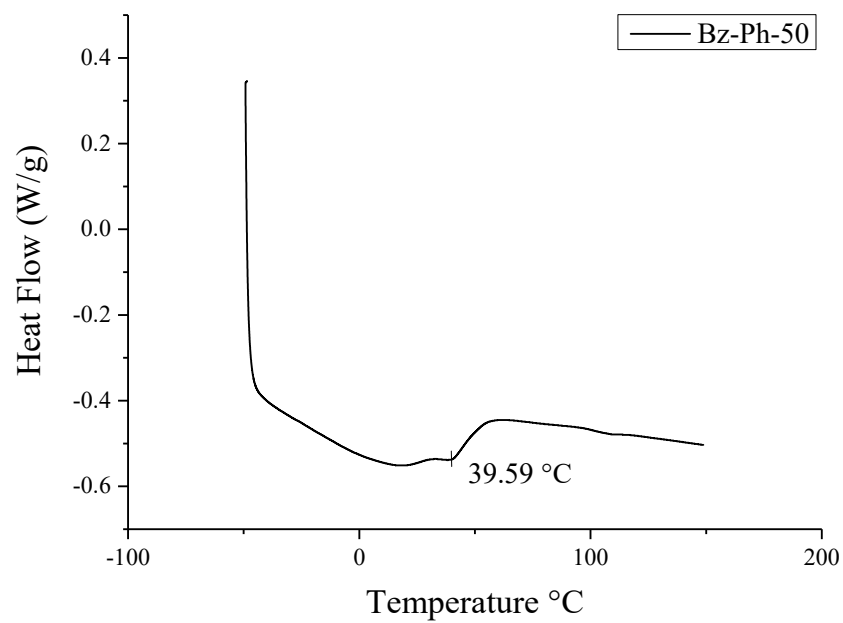


**Figure S43.** DSC of the polymer from table 1, entry 5.



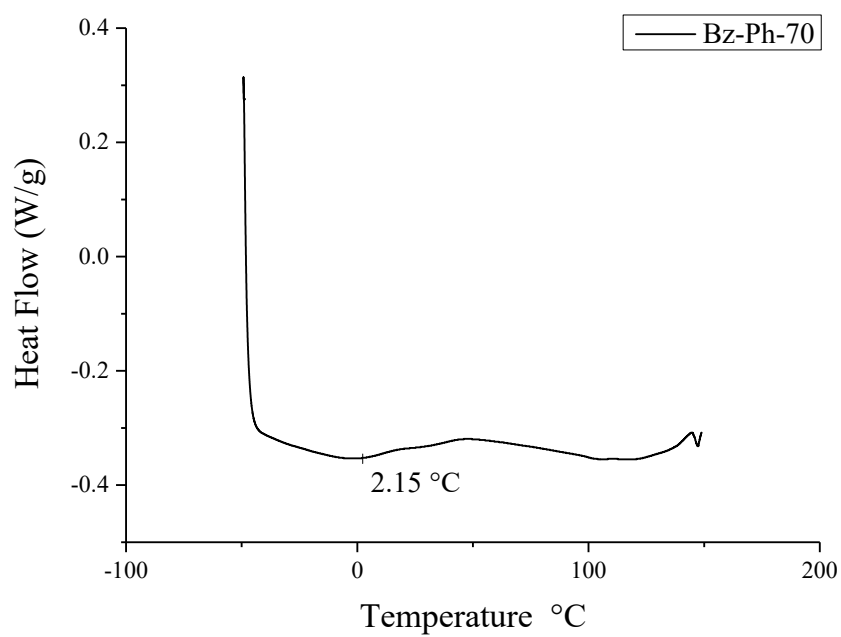


**Figure S44.** DSC of the polymer from table 1, entry 6.

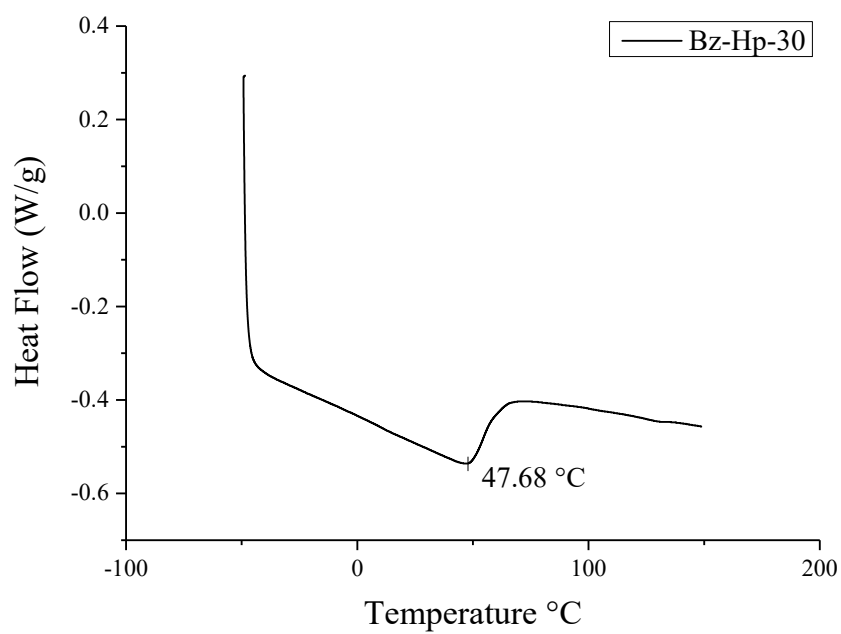


**Figure S45.** DSC of the polymer from table 1, entry 7.

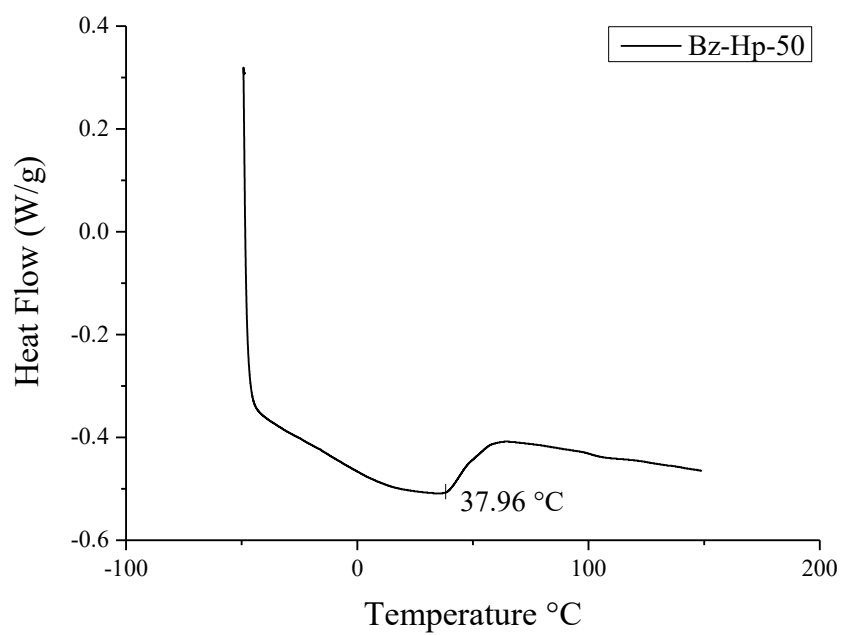


**Figure S46.** DSC of the polymer from table 1, entry 8.

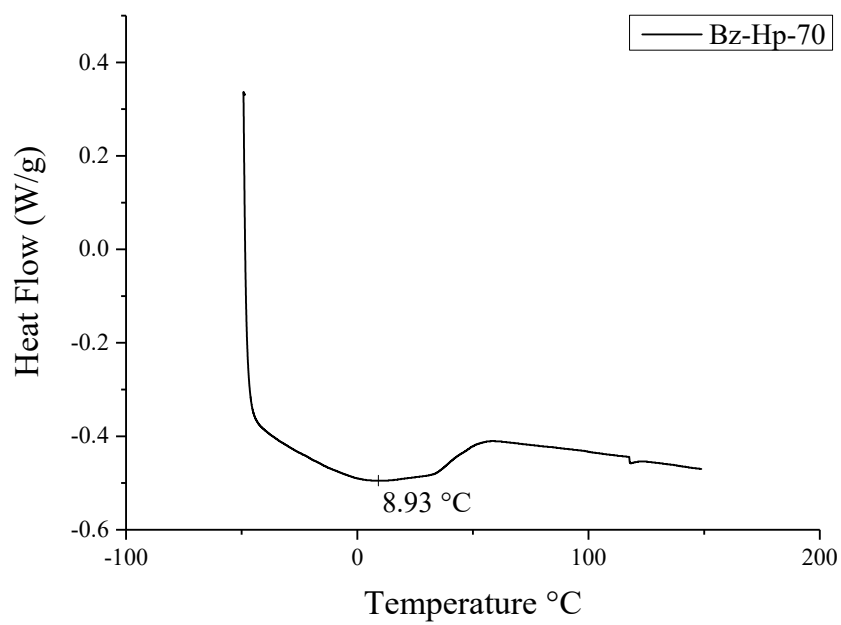
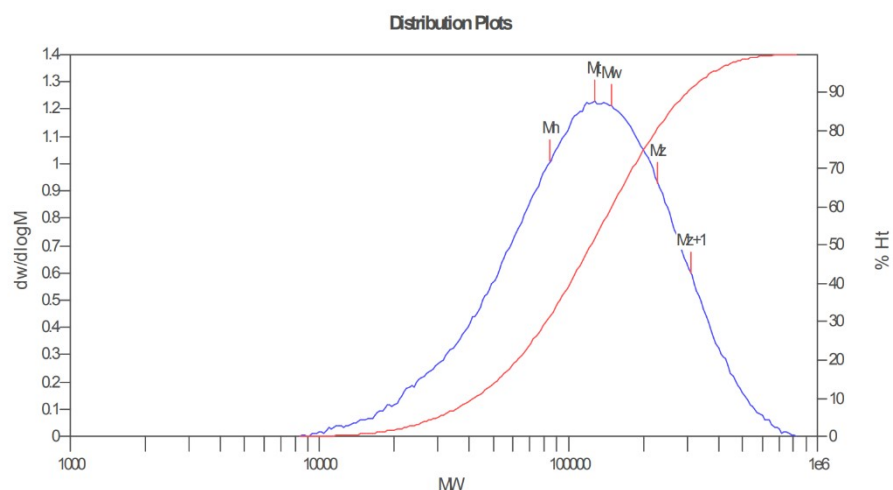


**Figure S47.** DSC of the polymer from table 1, entry 9.



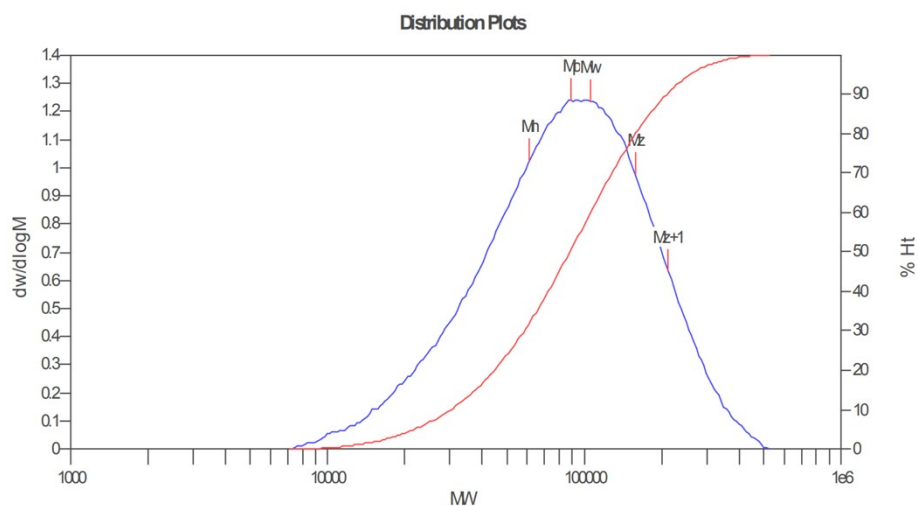
#### MW Averages

| Peak No | Mp     | Mn    | Mw     | Mz     | Mz+1   | Mv     | PD      |
|---------|--------|-------|--------|--------|--------|--------|---------|
| 1       | 126943 | 84420 | 149456 | 228583 | 310452 | 138960 | 1.77039 |

#### Processed Peaks

| Peak No | Name | Start RT (mins) | Max RT (mins) | End RT (mins) | Pk Height (mV) | % Height | Area (mV.secs) | % Area |
|---------|------|-----------------|---------------|---------------|----------------|----------|----------------|--------|
| 1       |      | 12.18           | 13.57         | 15.58         | 3.08981        | 0        | 257.253        | 100    |

**Figure S48.** GPC of the polymer from table 1, entry 4.



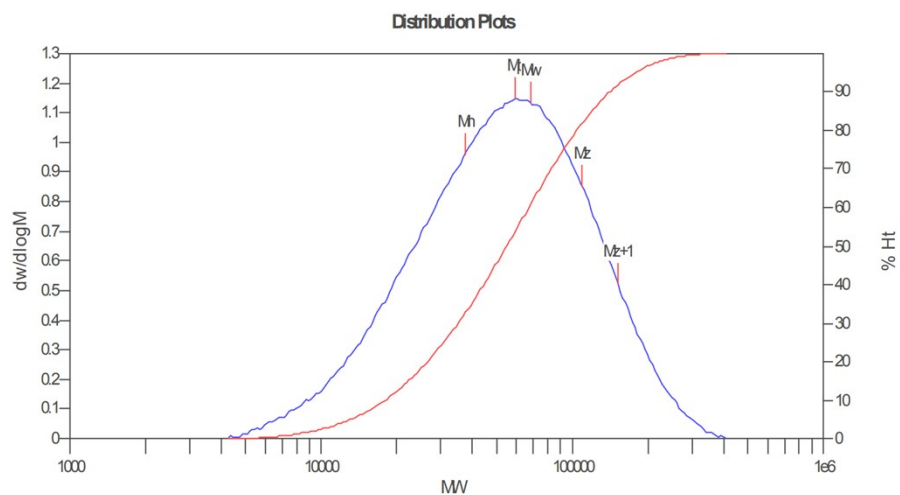
#### MW Averages

| Peak No | Mp    | Mn    | Mw     | Mz     | Mz+1   | Mv    | PD      |
|---------|-------|-------|--------|--------|--------|-------|---------|
| 1       | 88556 | 61135 | 105367 | 158098 | 211301 | 98270 | 1.72351 |

#### Processed Peaks

| Peak No | Name | Start RT (mins) | Max RT (mins) | End RT (mins) | Pk Height (mV) | % Height | Area (mV.secs) | % Area |
|---------|------|-----------------|---------------|---------------|----------------|----------|----------------|--------|
| 1       |      | 12.52           | 13.83         | 15.70         | 3.72485        | 0        | 306.485        | 100    |

**Figure S49.** GPC of the polymer from table 1, entry 5.



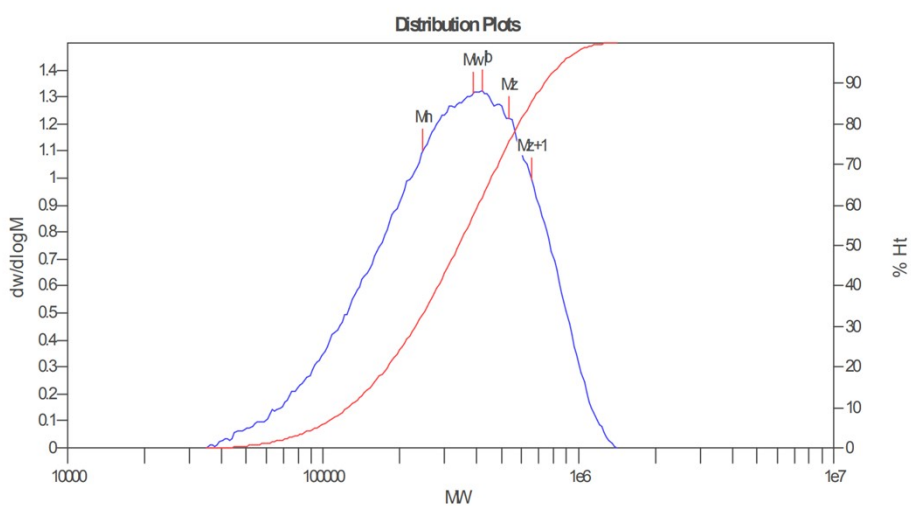
**MW Averages**

| Peak No | Mp    | Mn    | Mw    | Mz     | Mz+1   | Mv    | PD      |
|---------|-------|-------|-------|--------|--------|-------|---------|
| 1       | 59057 | 37334 | 68610 | 109446 | 152442 | 63333 | 1.83774 |

**Processed Peaks**

| Peak No | Name | Start RT (mins) | Max RT (mins) | End RT (mins) | Pk Height (mV) | % Height | Area (mV.secs) | % Area |
|---------|------|-----------------|---------------|---------------|----------------|----------|----------------|--------|
| 1       |      | 12.70           | 14.13         | 16.08         | 3.80998        | 0        | 339.957        | 100    |

**Figure S50.** GPC of the polymer from table 1, entry 6.



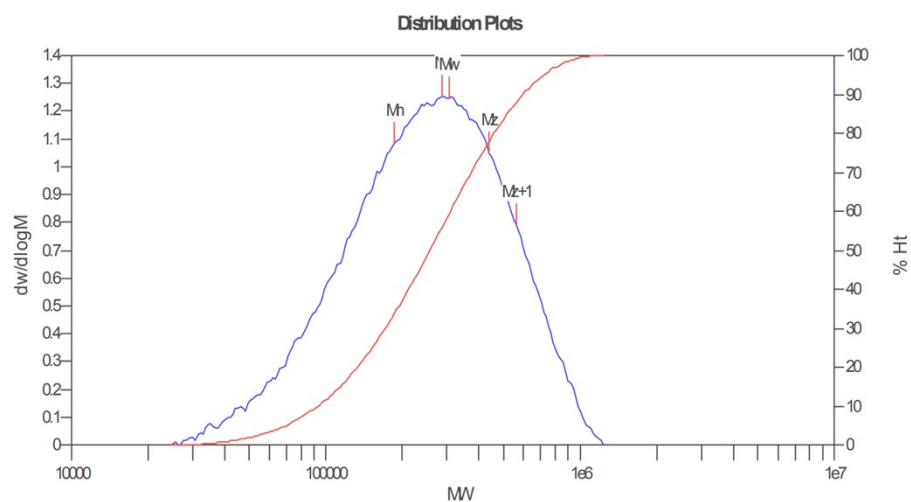
**MW Averages**

| Peak No | Mp     | Mn     | Mw     | Mz     | Mz+1   | Mv     | PD      |
|---------|--------|--------|--------|--------|--------|--------|---------|
| 1       | 418466 | 246438 | 386210 | 531314 | 657352 | 365079 | 1.56717 |

**Processed Peaks**

| Peak No | Name | Start RT (mins) | Max RT (mins) | End RT (mins) | Pk Height (mV) | % Height | Area (mV.secs) | % Area |
|---------|------|-----------------|---------------|---------------|----------------|----------|----------------|--------|
| 1       |      | 11.78           | 12.68         | 14.52         | 2.36463        | 0        | 182.76         | 100    |

**Figure S51.** GPC of the polymer from table 1, entry 7.



#### MW Averages

| Peak No | Mp     | Mn     | Mw     | Mz     | Mz+1   | Mv     | PD      |
|---------|--------|--------|--------|--------|--------|--------|---------|
| 1       | 285426 | 185372 | 303465 | 437466 | 561382 | 284769 | 1.63706 |

#### Processed Peaks

| Peak No | Name | Start RT (mins) | Max RT (mins) | End RT (mins) | Pk Height (mV) | % Height | Area (mV.secs) | % Area |
|---------|------|-----------------|---------------|---------------|----------------|----------|----------------|--------|
| 1       |      | 11.88           | 12.97         | 14.78         | 1.95501        | 0        | 159.711        | 100    |

**Figure S52.** GPC of the polymer from table 1, entry 8.

### 3. References

1. Y. Ge, S. Li, W. Fan and S. Dai, Flexible "Sandwich" (8-Alkyl-naphthyl  $\alpha$ -Diimine) Catalysts in Insertion Polymerization, *Inorganic Chemistry*, 2021, **60**, 5673-5681.

### 4. X-ray Crystallography

| Table S1 Crystal data and structure refinement for Pd1. |  |
|---|--|
| Identification code                                     | <b>Pd1</b>   |
| Empirical formula                                       | C <sub>25</sub> H <sub>23</sub> Cl N <sub>2</sub> Pd |
| Formula weight  | 493.30   |
| Temperature/K   | 298(2)   |
| Crystal system  | Triclinic  |
| Space group   | P-1  |
| a/Å   | 8.2420(8)  |
| b/Å   | 9.4049(9)  |
| c/Å   | 15.0201(14)  |
| $\alpha$ /°   | 103.390(3)   |
| $\beta$ /°  | 98.220(2)  |
| $\gamma$ /°   | 103.075(3)   |

|   |   |
|---|---|
| Volume/Å <sup>3</sup>                       | 1079.57(18)                                 |
| Z   | 2   |
| $\rho_{\text{calc}}/\text{cm}^3$            | 1.518                                       |
| $\mu/\text{mm}^{-1}$                        | 0.997                                       |
| F(000)                                      | 500   |
| Crystal size/mm <sup>3</sup>                | 0.30 x 0.27 x 0.13                          |
| 2 $\Theta$ range for data collection/°      | 2.31 to 25.02                               |
| Index ranges                                | -9<= $h$ <=9, -11<= $k$ <=9, -17<= $l$ <=13 |
| Reflections collected                       | 5234  |
| Independent reflections                     | 3731 [R(int) = 0.0373]                      |
| Data/restraints/parameters                  | 3731 / 6 / 266                              |
| Goodness-of-fit on F <sup>2</sup>           | 1.060                                       |
| Final R indexes [ $I \geq 2\sigma(I)$ ]     | R1 = 0.0626, wR2 = 0.1731                   |
| Final R indexes [all data]                  | R1 = 0.0698, wR2 = 0.1800                   |
| Largest diff. peak/hole / e Å <sup>-3</sup> | 1.850 and -1.938                            |

| <b>Table S2 Crystal data and structure refinement for Pd2.</b> |  |
|--|--|
| Identification code  | <b>Pd2</b>                                 |
| Empirical formula  | C51 H43 Cl N2 Pd                           |
| Formula weight   | 825.72                                     |
| Temperature/K  | 298(2)                                     |
| Crystal system   | Triclinic                                  |
| Space group  | P-1  |
| a/Å  | 7.9650(8)                                  |
| b/Å  | 11.2240(12)                                |
| c/Å  | 27.180(3)                                  |
| $\alpha/^\circ$  | 92.890(2)                                  |
| $\beta/^\circ$   | 95.260(3)                                  |
| $\gamma/^\circ$  | 106.440(4)                                 |
| Volume/Å <sup>3</sup>  | 2313.3(4)                                  |
| Z  | 2  |
| $\rho_{\text{calc}}/\text{cm}^3$                               | 1.185                                      |
| $\mu/\text{mm}^{-1}$   | 0.492                                      |
| F(000)   | 852  |
| Crystal size/mm <sup>3</sup>                                   | 0.11 x 0.08 x 0.03                         |
| 2 $\Theta$ range for data collection/°                         | 1.90 to 25.02                              |
| Index ranges   | -9<= $h$ <=9, -13<= $k$ <=13, 0<= $l$ <=32 |
| Reflections collected  | 7920                                       |
| Independent reflections  | 7920 [R(int) = 0.0000]                     |

|  |                           |
|--|---------------------------|
| Data/restraints/parameters                     | 7920 / 234 / 499          |
| Goodness-of-fit on $F^2$                       | 1.089                     |
| Final R indexes [ $I \geq 2\sigma(I)$ ]        | R1 = 0.1660, wR2 = 0.3410 |
| Final R indexes [all data]                     | R1 = 0.3004, wR2 = 0.3908 |
| Largest diff. peak/hole / $e \text{ \AA}^{-3}$ | 1.178 and -0.986          |